© 2018. Published by The Company of Biologists Ltd | Development (2018) 145, dev162529. doi:10.1242/dev.162529

RESEARCH ARTICLE

The LPA-LPA4 axis is required for establishment of bipolar morphology and radial migration of newborn cortical neurons

Nobuhiro Kurabayashi[1], Aiki Tanaka[1], Minh Dang Nguyen[2] and Kamon Sanada[1,*]

ABSTRACT

Newborn neurons in the developing neocortex undergo radial migration, a process that is coupled with their precise passage from multipolar to bipolar shape. The cell-extrinsic signals that govern this transition are, however, poorly understood. Here, we find that lysophosphatidic acid (LPA) signaling contributes to the establishment of a bipolar shape in mouse migratory neurons through LPA receptor 4 (LPA4). LPA4 is robustly expressed in migratory neurons. LPA4-depleted neurons show impaired multipolar-to-bipolar transition and become arrested in their migration. Further, LPA4-mediated LPA signaling promotes formation of the pia-directed process in primary neurons overlaid on neocortical slices. In addition, LPA4 depletion is coupled with altered actin organization as well as with destabilization of the F-actin-binding protein filamin A (FlnA). Finally, overexpression of FlnA rescues the morphology and migration defects of LPA4-depleted neurons. Thus, the LPA-LPA4 axis regulates bipolar morphogenesis and radial migration of newborn cortical neurons via remodeling of the actin cytoskeleton.

KEY WORDS: Developing neocortex, G-protein-coupled receptor, Lysophosphatidic acid, Neuronal migration, Mouse

INTRODUCTION

Development of the mammalian cerebral cortex is achieved by the intervention of a series of cellular events including neurogenesis, neuronal migration and neuronal maturation. Neuronal migration is a fundamental process for establishing the laminated structure of the cerebral cortex (Ayala et al., 2007; Cooper, 2014; Evsyukova et al., 2013; Kriegstein and Noctor, 2004; Marín et al., 2010; Tsai and Gleeson, 2005). In the developing neocortex, neurons are born from neural progenitor cells/intermediate progenitor cells residing at the ventricular zone/subventricular zone (VZ/SVZ). Newborn neurons initially show a multipolar morphology in the SVZ and lower IZ (LoTurco and Bai, 2006; Marín et al., 2010; Noctor et al., 2004; Tabata and Nakajima, 2003). Subsequently, they extend a ventricle-directed thin tailing process (axon), reorient their centrosomes and Golgi toward the pia in accordance with their radial polarization, and form a single pia-directed thick process (leading process) to adopt a bipolar shape. Neurons with bipolar shape in the lower IZ thereafter exit the IZ and move radially toward the pial surface. These processes of radial polarization and morphological transformation most likely depend on the coordinated actions of extracellular factors and intracellular signaling. To date, only the extracellular glycoprotein reelin and guidance cue semaphorin 3A have been shown to promote the multipolar-to-bipolar transition of newborn neurons through induction of radial polarization (Cooper, 2014; Evsyukova et al., 2013; Marín et al., 2010). However, the extracellular signals and downstream pathways that remodel the cytoskeleton to control morphological transformation of newborn neurons remain largely unknown.

Lysophosphatidic acid (LPA) is a bioactive lipid molecule composed structurally of a phosphate, a glycerol and a fatty acid (Tokumura, 1995). The extracellular actions of LPA are mediated by at least 6 subtypes of G-protein-coupled receptors referred to as LPA1 to LPA6 (Yung et al., 2015). LPA1, LPA2 and LPA4 are known to express in murine embryonic brains (Choi et al., 2010; Yung et al., 2015). Both LPA1 and LPA2 are reported to play a role in neural progenitor cells (Choi et al., 2010; Fukushima et al., 2007; Kingsbury et al., 2003). On the other hand, the roles of LPA4 in the developing brain remain unclear, as mice deficient for LPA4 show normal gross brain anatomy but this may be due to compensatory effects (Lee et al., 2008; Sumida et al., 2010).

In the present study, we find that LPA4 is expressed in migratory neurons of the mouse developing neocortex. Depletion of LPA4 in neurons profoundly impairs neuronal migration and accumulates multipolar neurons in the lower IZ. Using neuronal culture system, we discovered that LPA4-depleted neurons display normal apical localization of the centrosome/Golgi, but fail to form the pia-directed process. Therefore, they remain in a multipolar state, instead of adopting a bipolar morphology. Conversely, LPA treatment leads to precocious formation of the pia-directed process through LPA4, and this morphological change is accompanied with aberrant neuronal migration. Furthermore, LPA4 depletion is coupled with altered remodeling of the actin cytoskeleton, as well as with destabilization of the F-actin-binding protein filamin A (FlnA). Finally, FlnA overexpression rescues defects in remodeling of the actin cytoskeleton, formation of the pia-directed process and neuronal migration of LPA4-depleted neurons.

RESULTS

LPA4 is expressed in the developing neocortex

We first localized LPA4 in the mouse developing neocortex. As shown in Fig. 1A, LPA4 immunoreactivity was prominent at embryonic day (E) 14 and E17, from mid to late corticogenesis. However, no immunoreactivity was detected at E11, whereas reduced signal was detected at postnatal day (P) 1 (Fig. 1A). At E14 and E17, LPA4 immunoreactivity was enriched in the cortical plate (CP) and intermediate zone (IZ), where migratory neurons are abundant (Fig. 1A,B). In addition, relatively weaker LPA4 immunoreactivity was detected in the ventricular zone (VZ) where neural progenitor cells reside. Within the IZ and CP, LPA4

[1]Molecular Genetics Research Laboratory, Graduate School of Science, The University of Tokyo, Hongo 7-3-1, Bunkyo-ku, Tokyo 113-0033, Japan. [2]Hotchkiss Brain Institute, University of Calgary, Departments of Clinical Neurosciences, Cell Biology and Anatomy, Biochemistry and Molecular Biology, 3330 Hospital Drive NW, HMR 151, Calgary, Alberta T2N4N1, Canada.

*Author for correspondence (kamon_sanada@gen.s.u-tokyo.ac.jp)

N.K., 0000-0003-3097-8539; K.S., 0000-0002-0280-8957

Received 15 December 2017; Accepted 30 July 2018

Development (2018) 145, dev162529. doi:10.1242/dev.162529

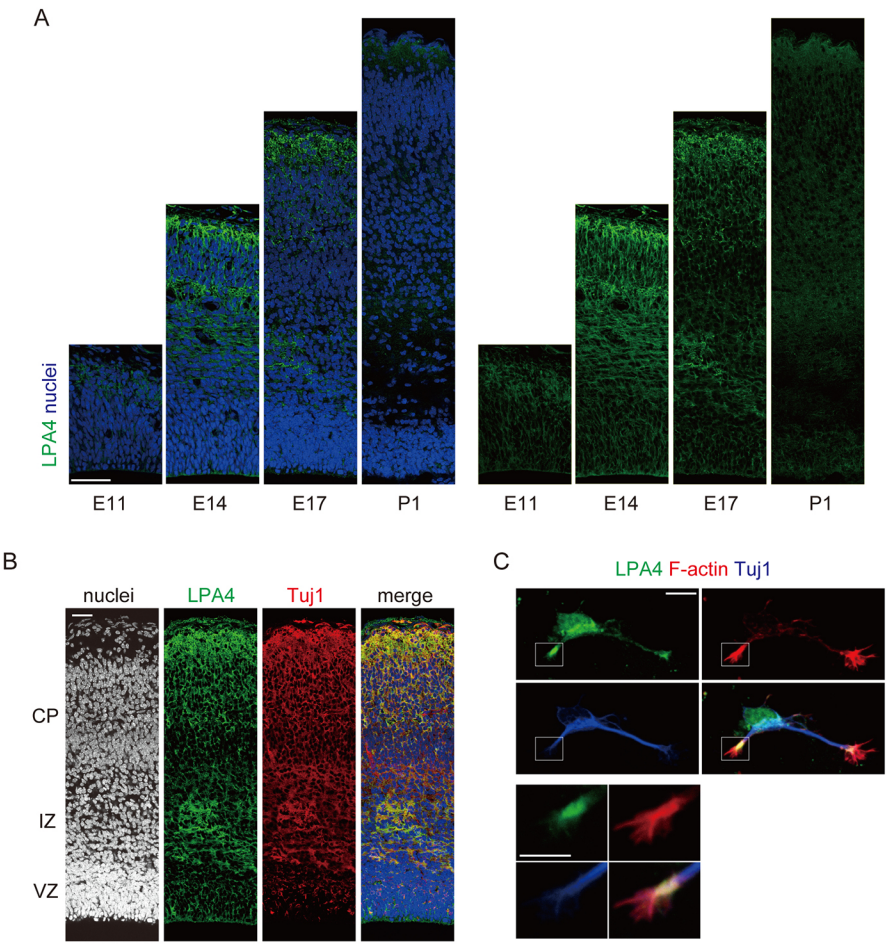

Fig. 1. Expression of LPA4 in the developing neocortex. (A) Neocortical coronal sections (E11, E14, E17 and P1) immunostained using anti-LPA4 antibody. Images of the entire cerebral wall are shown. Nuclei were stained with TO-PRO-3 iodide. (B) E17 neocortical coronal sections immunostained using anti-LPA4 (green) and Tuj1 (red) antibodies. Images of the entire cerebral wall are shown. (C) Neocortical neurons at 2 DIV were immunostained using antibodies against LPA4 (green) and Tuj1 (blue). F-actin was stained with actistain phalloidin. Magnified images of the boxed areas are shown in the lower panels. Scale bars: 50 µm in A; 25 µm in B; 10 µm in C; 5 µm in magnified images in C.

immunoreactivity showed remarkable overlapping expression with the neuronal marker Tuj1. As almost no immunoreactivity was observed in brain sections immunostained using LPA4 antibody pre-absorbed with its immunogen (Fig. S1A), these observations together indicate that LPA4 is expressed in migratory/maturating neurons and to a lesser extent in neural progenitor cells. In addition, in cultured cortical neurons prepared from the E14 neocortex, LPA4 immunoreactivity was detected throughout cell soma and enriched in tips of neurites (Fig. 1C). Specificity of the immunostaining signals was confirmed by the diminished LPA4 immunoreactivity in primary neurons depleted of the LPA4 protein by RNAi (Fig. S1D,E; see below), further supporting the neuronal expression of LPA4.

LPA4-depleted neurons show impaired multipolar-to-bipolar transition and arrest their migration *in vivo*

To characterize the functions of LPA4 in migratory neurons in the developing neocortex, we used DNA-based RNAi approach to acutely knock down the expression of LPA4. For this, we generated plasmids expressing two different short hairpin RNAs (shRNA) against LPA4 (LPA4 shRNA#1 and shRNA#2). These shRNA constructs efficiently silenced LPA4 overexpressed in HEK cells (Fig. S1B). In addition, the shRNA constructs diminished endogenous levels of LPA4 in NIH3T3 cells and primary neurons (Fig. S1C-E). We then electroporated the LPA4 shRNA constructs together with the GFP-expression construct into E14 neocortices to knockdown LPA4 in migratory neurons. In E17 neocortices electroporated with the control shRNA at E14, the majority of the GFP-labeled neurons migrated into the CP and a smaller population of the cells were detected in the IZ. On the other hand, in LPA4 shRNA-introduced neocortices, most of the GFP-labeled cells were located at the interface between the VZ and IZ, and a small population of the cells resided into the CP (Fig. 2A,B). Noticeably, control GFP-positive cells around the lower IZ showed a typical bipolar morphology or a unipolar morphology with a pia-directed process but no detectable tailing process (Fig. 2C,D). On the other hand, most of the LPA4 shRNA-introduced neurons in the lower IZ had multiple short thin processes, or displayed no detectable processes (Fig. 2C,D). The defects in neuronal morphology and positioning of LPA4 shRNA#1-introduced neocortices are almost completely rescued by expression of LPA4 with two silent mutations within the LPA4 shRNA#1 target sequence (LPA4-res; Fig. S1B). These observations not only confirm the specificity of LPA4 shRNA but also indicate that LPA4-depleted neurons display impaired multipolar-to-bipolar transition. As LPA4-depleted neurons are still mis-positioned at the subcortical region at P4 (Fig. 2E,F), we reason that LPA4 knockdown arrests (rather than delays) neuronal migration.

Of note, as in control neurons, almost all misplaced LPA4-depleted neurons were positive for Cux1, a marker of cells destined for layer 2-4 neurons (Nieto et al., 2004) (Fig. 2G). This observation suggests that laminar fate was not altered upon LPA4 depletion and consequently that alteration of laminar fate does not account for the mis-positioning of LPA4-depleted neurons. Nonetheless, immunofluorescent intensities of Cux1 in LPA4-depleted neurons were significantly lower than that in control GFP-labeled neurons

Development (2018) 145, dev162529. doi:10.1242/dev.162529

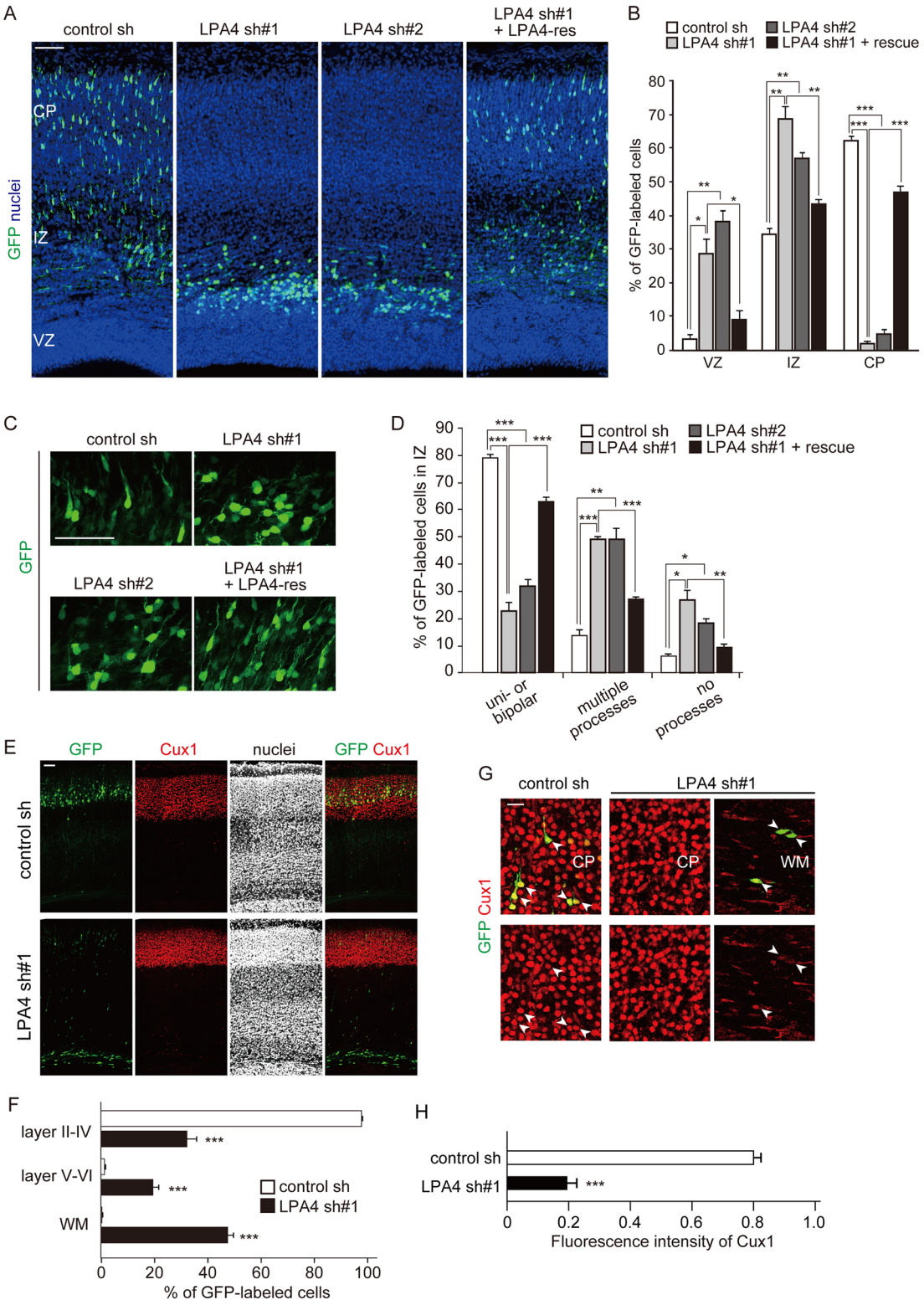

Fig. 2. See next page for legend.

(Fig. 2G,H). As Cux1 immunoreactivity is known to increase with neuronal maturation (Nieto et al., 2004), this observation suggests that maturation of LPA4-depleted neurons was likely delayed. In addition, mis-positioning of LPA4-depleted neurons was unlikely caused by disruption of the radial glial scaffold, as indicated by the normal radial fibers reaching the pia in LPA4 shRNA-introduced neocortices (Fig. S2). Neuronal differentiation of progenitor cells was also unaffected in LPA4-electroporated neocortices: the populations of GFP-labeled cells positive for Pax6 (a neural progenitor marker) and Tbr2 (an intermediate progenitor marker) were unchanged in E15 neocortices electroporated with LPA4 shRNA at E13 (Fig. S3). Finally, apoptosis was not enhanced

Development (2018) 145, dev162529. doi:10.1242/dev.162529

Fig. 2. Knockdown of LPA4 results in impaired neuronal migration and multipolar-to-bipolar transition. (A-D) Plasmids expressing control shRNA, LPA4 shRNAs and shRNA-resistant LPA4 (LPA4-res) as indicated were electroporated, together with a GFP-expressing plasmid, in E14 embryos. Embryos were harvested at E17. Brain sections were immunostained with antibody against GFP (green). Nuclei were stained with TO-PRO-3 iodide. (A) Representative images of GFP-labeled cells throughout the entire cerebral wall. (B) The percentage of GFP-labeled cells in the VZ, IZ and CP was calculated and is plotted as the mean±s.e.m. **P*<0.05, ***P*<0.01, ****P*<0.001 by one-way ANOVA followed by Bonferroni's multiple comparison test (*n*=3 or 4 brains; 1315, 1390, 819 and 1647 cells were counted for control, sh#1, sh#2 and sh#1+rescue, respectively). (C) Magnified images of GFP-labeled cells in the IZ. (D) The percentage of GFP-labeled neurons with uni- or bipolar morphology, multiple (≥3) minor processes or no processes in the IZ was calculated and is plotted as mean±s.e.m. **P*<0.05, ***P*<0.01, ****P*<0.001 by one-way ANOVA followed by Bonferroni's multiple comparison test (*n*=3 or 4 brains; 343, 317, 252 and 361 cells were counted for control, sh#1, sh#2 and sh#1+rescue, respectively.). (E-H) Plasmids expressing GFP and LPA4 shRNA were electroporated in E14 embryos, and the embryos were harvested at P4. Brain sections were immunostained using Cux1 antibodies. Nuclei were stained with TO-PRO-3 iodide. (E) Representative images of electroporated neocortical sections. (F) The percentage of GFP-labeled cells in the layers II-IV, layers V and VI, and white matter (WM) was calculated and is plotted as the mean±s.e.m. ****P*<0.001 by a two-tailed Student's *t*-test (*n*=3 brains, 297 and 361 cell were counted for control and sh#1, respectively). (G) High-magnification images of the CP region in the control neocortex (left panel) and CP (middle panel)/WM (right panel) regions in LPA4 shRNA-introduced neocortex. Arrowheads indicate GFP-labeled cells. (H) Immunofluorescence intensities of Cux1 in individual control GFP-positive cells and in nearby GFP-negative cells in the CP were measured, and the ratio of the intensity values is plotted. In addition, immunofluorescence intensities of Cux1 in LPA4-depleted cells in the WM and in GFP-negative cells in the CP were measured in the same brain section, and the ratio of the intensity values is also plotted. For quantification, Cux1 images were obtained using identical microscope settings. ****P*<0.001 by a two-tailed Welch's *t*-test (*n*=4 embryos, total 80-95 cells). Scale bars: 50 µm in A,C,E; 20 µm in G.

following LPA4 shRNA electroporation (Fig. S4). In summary, these results suggest that LPA4 is required for neurons to adopt a bipolar shape and to undergo radial migration.

LPA4 is required for formation of the pia-directed process in neurons

To further examine the effects of LPA4 knockdown on neuronal morphology, we used the slice overlay culture system (Polleux et al., 2000) in which dissociated GFP (or mCherry)-labeled cortical neurons are placed on neonatal cortical slices. In this particular system, cortical neurons prepared from E16 neocortices electroporated with GFP at E14 initially display multipolar morphology with short thin processes after ∼24 h in culture (Fig. 3A). After ∼2 days in culture, these neurons adopt a bipolar shape with a pia-directed thick process that is negative for the dendritic marker MAP2, and a ventricle-directed thin axon (Fig. 3A). The morphological transformation is reminiscent of that of migratory neurons *in vivo*. This system allows us to perform biochemical and molecular manipulations on growing neurons in an environment resembling the *in vivo* situation. By 5 days in culture, neurons on slices eventually differentiate into pyramidal neurons characterized by a single MAP2-positive pia-directed process, several basal processes and a ventricle-directed long axon (Fig. 3A; Polleux et al., 2000). Using this culture system, we first examined the effect of LPA4 knockdown on cell morphology. For this, E14 neocortices were electroporated with either control shRNA/mCherry or LPA4 shRNA/GFP into dorsal VZ progenitors, which eventually give rise to pyramidal neurons, and cortical cells were prepared at E16. The control shRNA/mCherry- and LPA4 shRNA/GFP-introduced neurons were then mixed and subjected to the slice overlay culture (Fig. 3A). After 2 days in culture, most of the control shRNA-introduced cells displayed a bipolar morphology characterized by a pia-directed thick process and a ventricle-directed axon (Fig. 3B,C). In contrast, electroporation of LPA4 shRNA plasmids resulted in a smaller population of GFP-labeled cells with bipolar morphology. Instead, most of the LPA4 shRNA-introduced cells displayed a multipolar morphology characterized by multiple thin processes emerging from the cell body (Fig. 3B,C). The defect in absence of pia-oriented process in LPA4 shRNA#1-treated neurons was alleviated with expression of LPA4-res (Fig. 3D). Of note, most LPA4 knocked down neurons extended a single ventricle-directed axon-like process (96.3+0.47% in control sh versus 95.5+1.13% in LPA4 sh#1), although the length of the process was shorter than that of control neurons (Fig. S5).

The secreted factors Sema3A and reelin have been shown to influence to the radial polarization of multipolar neurons in the developing cortex by reorienting the centrosome/Golgi apparatus (Chen et al., 2008; Jossin and Cooper, 2011; Shelly et al., 2011). We sought to determine the orientation of the centrosomes and Golgi in multipolar neurons depleted of LPA4. As shown in Fig. 4, LPA4 depletion by shRNA did not affect formation of a ventricle-directed axon-like process nor did it alter the normal apical localization of the centrosome (Fig. 4A,B). The normal apical positioning of the centrosome/Golgi in LPA4-depleted multipolar neurons was also observed *in vivo* (Fig. 4C-F). Together, these results suggest that LPA4-depleted neurons normally orient the centrosomes and Golgi but fail to form the pia-directed process.

Alterations in LPA signaling affect formation of the pia-directed process

Given that LPA4 affects the multipolar-to-bipolar transition, we next assessed the effects of LPA ligands on the establishment of bipolar morphology. Using slice overlay culture system, we found that LPA supplementation (36 h) increases the fraction of neurons with bipolar morphology in a dose-dependent manner (Fig. 5A). Importantly, the increase was totally abolished upon LPA4 knockdown (Fig. 5A), thereby indicating that the effect of LPA treatment on the pia-directed process formation is mediated by LPA4. To further support the notion that LPA is responsible for establishment of bipolar morphology, we investigated the effects of perturbing LPA synthesis. LPA is mainly produced via two pathways (Aoki et al., 2008): by hydrolysis of phosphatidic acids by phospholipase A1 (PLA1) and A2 (PLA2); or via hydrolysis of lysophospholipids by the secreted enzyme lysophospholipase D (autotaxin; ATX). In the latter pathway, lysophospholipids are produced by phospholipase A1 (PLA1) and A2 (PLA2)-dependent hydrolysis of phospholipids predominantly present within cell membranes (Aoki et al., 2008). We first applied methyl arachidonyl fluorophosphonate (MAFP), an inhibitor for PLA1 and PLA2 (Higgs and Glomset, 1996; Lucas and Dennis, 2005), in a slice overlay culture system. The addition of MAFP (48 h) dramatically reduced the fraction of neurons with a pia-directed thick process (Fig. 5B). Noticeably, as co-treatment of MAFP with LPA almost completely reversed the impaired morphology of neurons observed with MAFP application, we reasoned that MAFP-induced impairment of the pia-directed process formation was attributable to inhibition of LPA synthesis. Next, we performed experiments in the presence of the potent ATX blockers HA155 and PF8380 (Albers et al., 2010; Gierse et al., 2010). We found that these inhibitors significantly reduced the proportion of neurons with bipolar morphology (Fig. 5C). In summary, interfering with

Development (2018) 145, dev162529. doi:10.1242/dev.162529

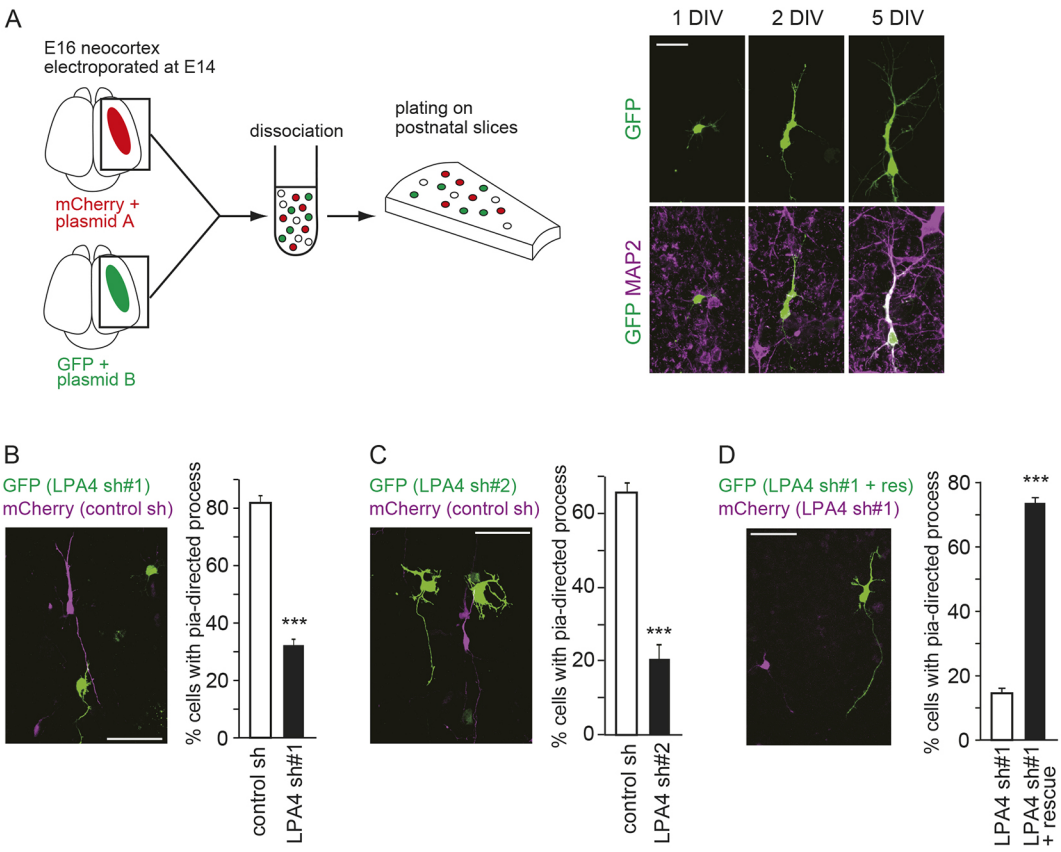

Fig. 3. LPA4 is required for formation of the pia-directed process in neurons. (A) The diagram illustrates the procedure for slice overlay culture of plasmid-introduced neurons (left). Representative images of GFP-labeled neurons growing over the cortical slices for the indicated time periods (right panels). The culture was immunostained using anti-MAP2 antibody. (B-D) Representative images of GFP neurons and mCherry neurons cultured on the CP of cortical slices for 48 h. Neurons were electroporated with the plasmids indicated. Percentages of cells with the pia-directed process in the total mCherry-labeled cells or GFP-labeled cells at the CP were calculated and are shown on the right. Data are presented as mean±s.e.m. ***P<0.001 by a two-tailed Student's t-test (n=5 or 6 slice cultures from two independent experiments). Scale bars: 20 µm in A; 50 µm in B-D.

LPA-LPA4 pathway impairs formation of the pia-directed process in neurons, whereas LPA treatment promotes its formation.

Pharmacological modifications of LPA signaling affect radial migration

Given that LPA supplementation and inhibition of LPA synthesis affect morphological transformation of cortical neurons in the slice overlay culture system, we next determined whether these manipulations can alter migration of cortical neurons. For this purpose, neocortical slices were prepared from E16 neocortices electroporated with GFP at E14 and cultured in the presence of LPA and/or inhibitors for LPA synthesis for 36 h. When compared with the distribution of the GFP-labeled cells in control-treated GFP-electroporated slices, a significantly larger fraction of the GFP cells was found at the upper part of the neocortices treated with LPA (Fig. 6A). In addition, more GFP-positive cells in the IZ exhibited the pia-directed thick process in the presence of LPA (Fig. 6B). On the other hand, MAFP treatment resulted in a smaller fraction of GFP cells positioned at the upper part of the neocortex as well as in a smaller fraction of GFP cells with the pia-directed thick process. Importantly, the mis-positioning and attenuated morphological transformation of these neurons were reversed with LPA (Fig. 6A,B). Similar to MAFP, PF8380 treatment of cortical slices resulted in impaired neuronal migration and morphology, and co-treatment with MAFP and PF8380 worsened the defects in neuronal positioning and morphology (Fig. 6C,D). Taken together, these results reveal that manipulations of LPA signaling have a significant impact on radial migration and neuronal morphology. They are consistent with our findings of altered multipolar-to-bipolar transformation and arrested neuronal migration in LPA4-depleted neocortices.

To further confirm the distinct role of LPA-LPA4 signaling in neuronal migration, we treated LPA4 shRNA-electroporated cortical slices with LPA or MAFP, and examined their effect on neuronal positioning. We found that neither LPA nor MAFP had significant effect on the cell positioning in LPA4-depleted cells (Fig. S6). This result indicates that LPA4 is the primary receptor for LPA signaling during neuronal migration in the developing neocortex.

LPA4 signaling affects the actin cytoskeleton

Based on the finding that the LPA-LPA4 axis contributes to neuronal morphogenesis, one can suspect that LPA signaling affects the cytoskeleton in newborn neurons. As remodeling of the actin filaments is central to cell morphogenesis, we sought to characterize the spatiotemporal formation of filamentous actin (F-actin) in neurons using the slice overlay culture system. To visualize F-actin, neurons co-transfected with GFP and the Lifeact peptide (an F-actin binding peptide; Riedl et al., 2008) tagged with DsRed were subjected to the slice overlay culture. As shown in Fig. 7, after 18 h in culture, almost all GFP-introduced neurons showed multipolar shape with intense F-actin signals (Lifeact-DsRed signals)

Development (2018) 145, dev162529. doi:10.1242/dev.162529

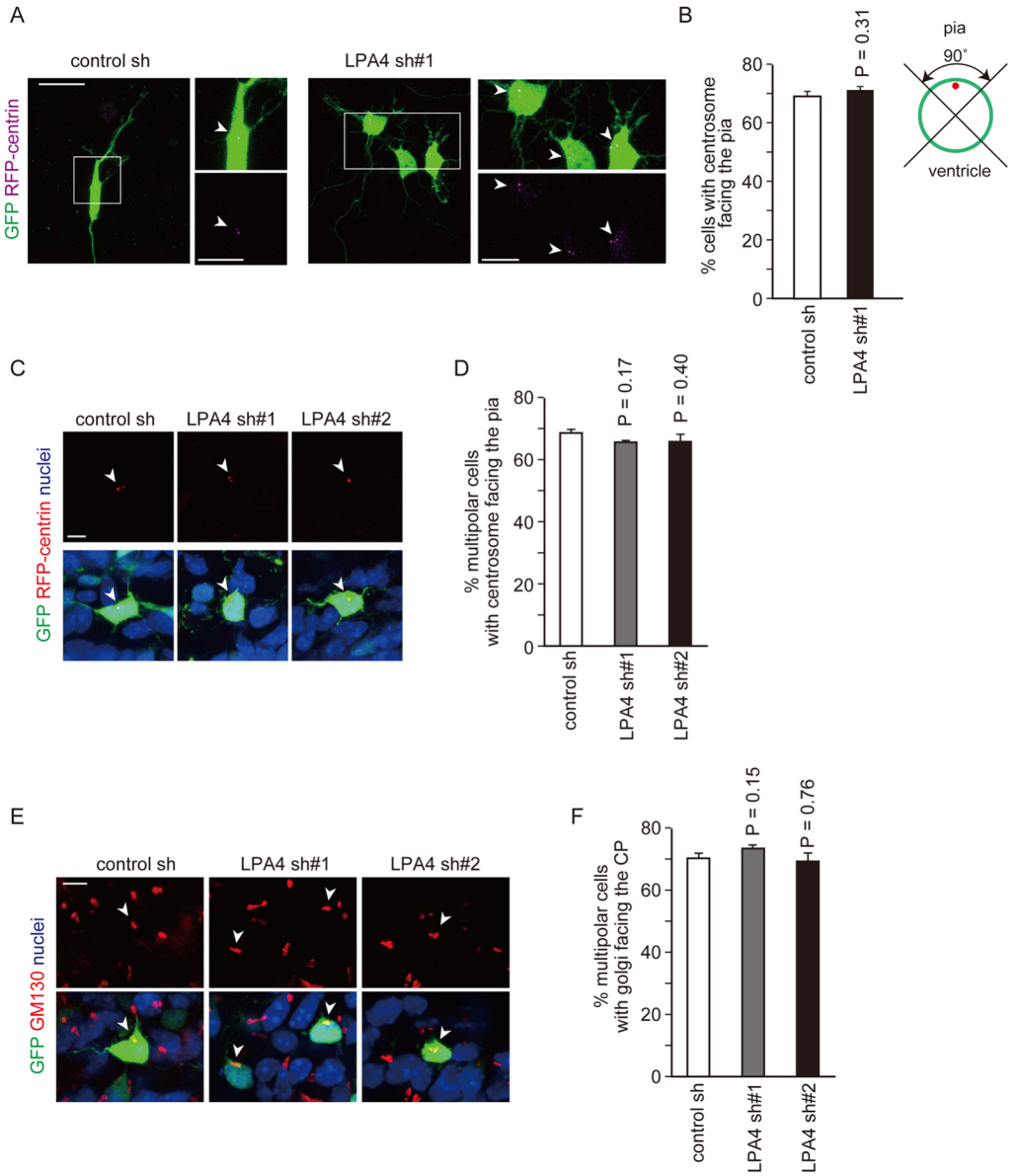

Fig. 4. The apical positioning of the centrosome/Golgi is not disrupted by LPA4 depletion. (A) Representative images of control and LPA4 shRNA-introduced neurons cultured on cortical slices for 2 days. Neurons were co-transfected with DsRed2-centrinII, a centrosome marker. Arrowheads indicate the position of the centrosome. (B) The percentage of GFP-labeled cells with the centrosome facing the pia was calculated and is plotted as mean ±s.e.m. (n=12 or 13 slice cultures from three independent experiments). (C,D) Plasmids expressing GFP, LPA4 shRNAs and DsRed2-CentinII were electroporated in E14 embryos, and the embryos were harvested at E16. (C) Representative images of GFP-labeled multipolar cells in the IZ. Arrowheads indicate the position of the centrosome. (D) The percentage of cells with the centrosome facing the pia in the total GFP-labeled multipolar cells in the IZ was calculated and is plotted as mean±s.e.m. (n=3 brains, 316, 253 and 360 cells were counted for control, sh#1 and sh#2, respectively). (E,F) Plasmids expressing GFP and LPA4 shRNAs were electroporated in E14 embryos, and the embryos were harvested at E16. (E) Representative images of GFP-labeled multipolar cells (immunostained with GM130, a Golgi marker) in the IZ. Arrowheads indicate the position of the Golgi apparatus. (F) The percentage of cells with Golgi facing the pia in the total GFP-labeled multipolar cells in the IZ was calculated and is plotted as mean±s.e.m. (n=3 brains, 240, 224 and 183 cells were counted for control, sh#1 and sh#2, respectively). Scale bars: 20 µm in A; 10 µm in magnified images in A; 5 µm in C,E.

distributed throughout the cell soma and in individual processes (Fig. 7A). After 48 h in culture, about one half of the neurons with multipolar shape showed F-actin signals distributed throughout the cell soma and in proximal parts of individual processes, similar to those at 18 h in culture. In contrast, the remaining half of the cells with multipolar shape displayed enrichment of F-actin signals at the apical side of the cell soma with reduced or no signal in individual processes (Fig. 7A). By contrast, almost all neurons with bipolar morphology showed F-actin signals accumulating at the apical compartment of the cell soma (at the base of the pia-directed process) (Fig. 7A). These observations suggest that in neurons with multipolar shape, F-actin is initially present throughout the cell soma and in individual processes. As differentiation proceeds, F-actin becomes enriched at the apical side beneath the to-be-extended pia-directed process. In support of the theory, time-lapse imaging also showed changes in distribution of Lifeact-DsRed from cell soma/neuritis to the apical compartment, prior to pia-directed process extension (Fig. S7).

Importantly, when LPA4-depleted neurons were cultured in the slice overlay culture system, a larger population of the cells showed widespread distribution of F-actin (14.7±1.7% in control sh versus 41.1±2.4% in LPA4 sh#1, P<0.001 by a two-tailed Student's t-test) (Fig. 7B,C) with no clear apical side enrichment of F-actin. These observations reveal that LPA4 depletion is coupled with altered remodeling of the actin cytoskeleton in neurons at multipolar stage.

Defects in LPA4-depleted neurons are rescued by filamin A overexpression

The F-actin-binding protein filamin A (FlnA) organizes the actin cytoskeleton and plays a key role in radial migration of neurons in the developing neocortex (Nagano et al., 2004; Razinia et al., 2012; Stossel et al., 2001). We found that FlnA signals were enriched at the apical side of the cell soma in multipolar cells that displayed F-actin enrichment (Fig. S8). Such enrichment of FlnA was not observed in multipolar cells with wide distribution of F-actin (Fig. S8). In addition, in cells with bipolar morphology, FlnA was distributed in the pia-directed process (Fig. S8). These results imply the involvement of FlnA in apical F-actin enrichment and pia-directed process formation. We observed a decrease in FlnA protein

Development (2018) 145, dev162529. doi:10.1242/dev.162529

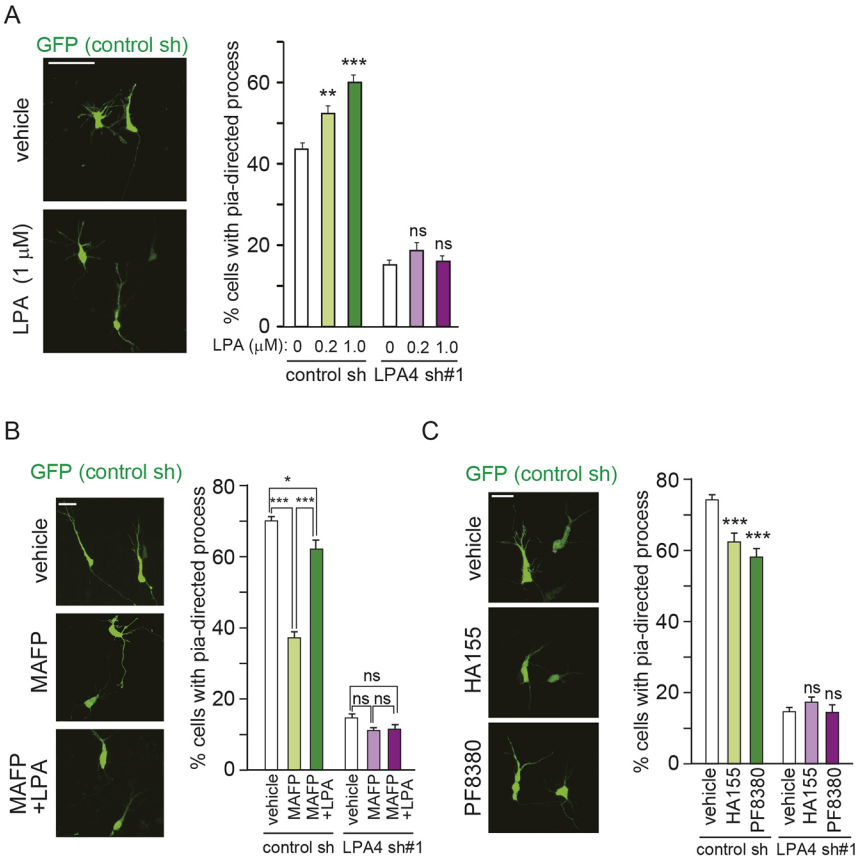

Fig. 5. Alterations in LPA signaling affect formation of the pia-directed process in neurons.
(A-C) Representative images of control shRNA-introduced GFP neurons cultured on the CP of cortical slices for 36 h (A) or 48 h (B,C) in the absence or presence of LPA (A), MAFP (B) or ATX inhibitors (C). The percentage of cells with the pia-directed process in the total GFP-labeled cells at the CP is shown on the right. The percentage of cells with the pia-directed process under LPA4 knockdown condition is also shown. Data are presented as mean±s.e.m. **P*<0.05, ***P*<0.01, ****P*<0.001 by one-way ANOVA followed by Bonferroni's multiple comparison test (B) or a two-tailed Student's *t*-test (A,C) (*n*=8-10 slice cultures from two independent experiments). Scale bars: 50 μm in A; 20 μm in B,C.

levels in cultured neurons prepared from E16 neocortices electroporated with LPA4 shRNA at E14, as assessed by immunostaining (Fig. 8A,B). We then sought to examine the potential effect of LPA4 knockdown on the stability of FlnA in NIH3T3 cells expressing HA-tagged FlnA. When compared with control, shRNA-introduced cells showing no significant decrease in FlnA levels; a large (~50%) decrease in FlnA levels was observed under LPA4-depleted condition and in the presence of CHX, a protein synthesis inhibitor (Fig. 8C,D). These results suggest that LPA4 signaling leads to stabilization of FlnA. In addition, in HEK293 cells, we found that FlnA associates with LPA4 (Fig. S9), suggesting that LPA4 localizes at close proximity to FLA through direct or indirect interaction; this may be important for stabilization of FlnA by LPA4.

We next investigated the potential link between FlnA- and LPA4-mediated pia-directed process formation of newborn neurons. We found that expression of a dominant-negative form of FlnA lacking the actin-binding domain (ΔABD-FlnA) produced fewer GFP-labeled cells with pia-directed process and apical enrichment of F-actin in the slice overlay culture system (Fig. 8E, Fig. S10), as did LPA4 depletion. In addition, the LPA-induced increase in the fraction of neurons with bipolar morphology was totally abolished upon ΔABD-FlnA expression (Fig. 8E). Furthermore, defects in actin reorganization and pia-directed process formation observed with LPA4 depletion were significantly rescued with expression of FinA (Fig. 8F). Importantly, expression of FlnA almost completely reversed the impaired neuronal positioning and morphology in LPA4 shRNA-depleted neocortices (Fig. 9). These findings indicate that pia-directed process malformation caused by LPA4 depletion is intimately coupled with the decreased levels of FlnA and impaired reorganization of the actin cytoskeleton.

DISCUSSION

The LPA-LPA4 axis contributes to morphological transformation and neuronal migration of newborn neurons

In the present study, we identify the LPA-LPA4 axis as an extrinsic signaling pathway required for the formation of the pia-directed process and hence for the establishment of bipolar morphology of cortical newborn neurons and for their radial migration. A previous report states that LPA inhibits migration of neurons (Fukushima et al., 2002). In the study, the authors showed that almost no neurons emerge from small pieces of cultured cortical explants in the presence of exogenous LPA. They also showed, in whole-brain culture, a marked difference in the distribution of β-tub III/Tuj1-positive cells following LPA application. However, as acknowledged by the authors, their observations cannot exclude the possibility that exogenous LPA alters neuronal processes other than migration per se (such as differentiation, survival, etc.) in the cortical cultures, thereby keeping neurons in the explant and changing the number of neurons produced and/or alive in the whole-brain culture (Fukushima et al., 2002; Kingsbury et al., 2003). In the present study, we directly examined the effects of LPA4 depletion, exogenous LPA and LPA synthesis inhibitors on neuronal migration in cortical slices. We found that migration of newborn neurons is promoted by exogenous LPA and retarded by LPA4 depletion and by LPA-synthesis inhibitors. Of note, maturation of LPA4-depleted neurons appears to be delayed, as indicated by the decreased levels of Cux1 (Fig. 2G,H). This is possibly due to the inappropriate environment surrounding the mis-positioned LPA4-depleted neurons. Alternatively, interference of LPA4 signaling may lead to cell-intrinsic defects in maturation programs. In these scenarios, altered migration of LPA4-depleted neurons may be partly attributable to delayed neuronal maturation.

Development (2018) 145, dev162529. doi:10.1242/dev.162529

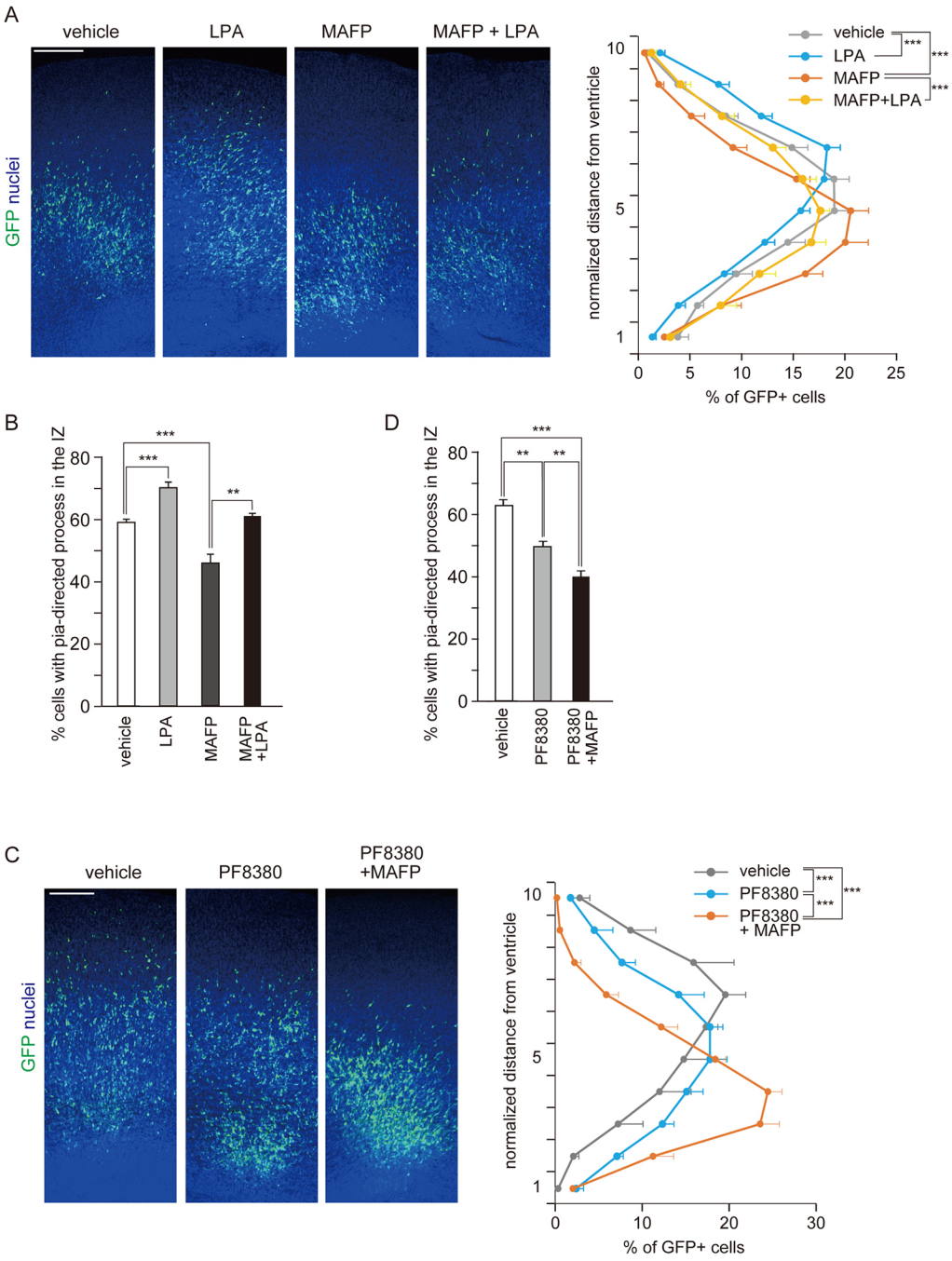

Fig. 6. LPA is required for proper neuronal morphology and migration in cultured cortical slices. (A-D) Plasmids expressing GFP were electroporated into E14 embryos. Acute brain slices were prepared from E16 brains and cultured for 36 h. The cultures were then immunostained using an antibody against GFP (green). Nuclei were stained with TO-PRO-3 iodide. (A,C) Representative images of GFP-labeled cells throughout the entire cerebral wall. Distributions of GFP-expressing cells along the radial axis under different treatments are shown on the right. ***P<0.001 by repeat measures two-way ANOVAs (n=4-9 slice cultures from at least two independent experiments). (B,D) The percentage of cells with the pia-directed process in the total GFP-labeled cells located in the IZ is shown. Data are presented as mean±s.e.m. **P<0.01, ***P<0.001 by a two-tailed Student's t-test (n=4-7 slice cultures from at least two independent experiments). Scale bars: 200 µm.

In the developing brain, LPA acts as a repellent factor for axons. In dispersed cortical neuron and retinal cultures, LPA causes axonal retraction (Fukushima et al., 2002; Campbell and Holt, 2003). In addition, LPA guides thalamocortical axons to proper cortical targets in brain slices (Cheng et al., 2016). In the present study, we uncovered a novel role for LPA signaling in the formation of the pia-directed process during the multipolar-to-bipolar transition. Thus, LPA mediates multiple context-dependent neuronal functions in the developing brain.

It is of note that mice with genetic deletion of *Lpa4* (*Lpar4* - Mouse Genome Informatics) show no overt phenotype during CNS development (Lee et al., 2008; Sumida et al., 2010), although the possibility of compensatory effects induced by genetic knockout cannot be excluded. This is reminiscent to the situation of *Lpa1*/*Lpa2* double-knockout mice that show mostly normal neocortical development (Contos et al., 2002), despite their potential involvement in progenitor biology. On the other hand, *in utero* electroporation of shRNA that allows the acute downregulation of genes, circumvents the compensatory mechanisms that may be activated in knockout animals [e.g. doublecortin (Bai et al., 2003), α-chimaerin (Ip et al., 2012) and β-amyloid precursor protein (Young-Pearse et al., 2007)]. This technique, combined with a RNAi approach enabled us to uncover novel function for LPA and LPA4 signaling in neuronal transformation and radial migration.

LPA-LPA4 signaling acts as a later morphogenic cue for newborn neurons

Sema3A and reelin have been reported to contribute to multipolar-to-bipolar transition of newborn neurons in the developing

Development (2018) 145, dev162529. doi:10.1242/dev.162529

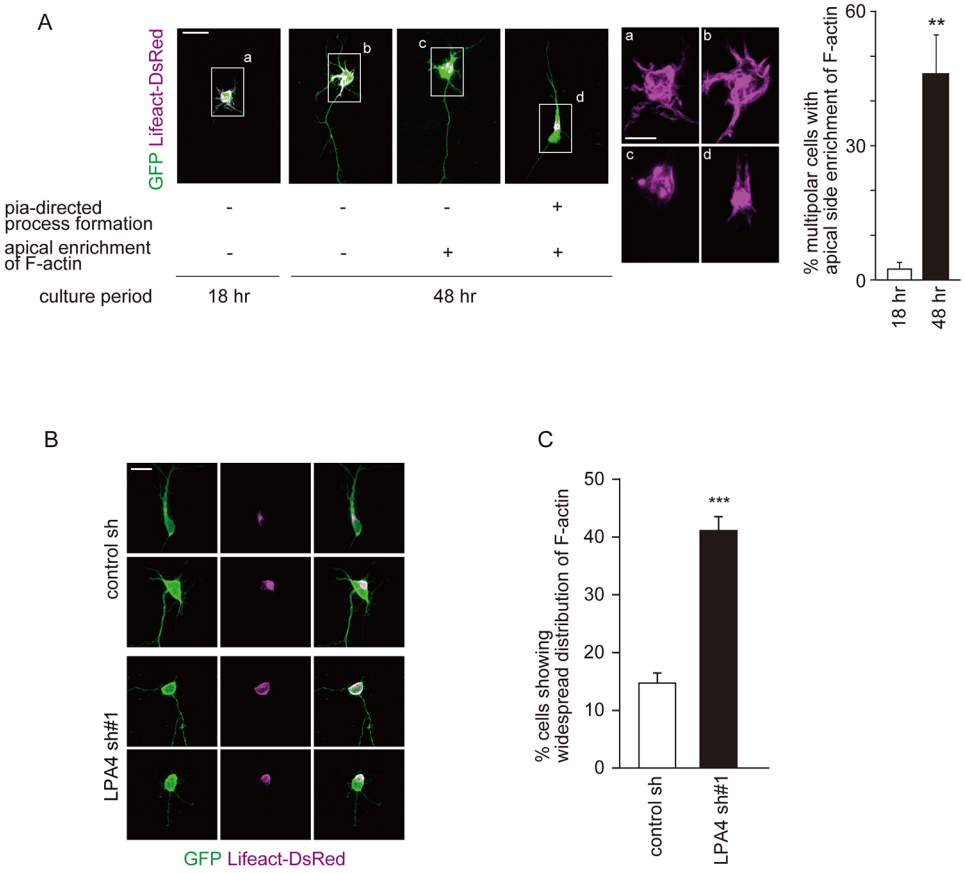

Fig. 7. LPA4 knockdown results in altered distribution of F-actin in neurons with multipolar shape. Plasmids expressing GFP- and Lifeact-DsRed were electroporated in E14 embryos. Neurons were prepared from E16 brains and subjected to a slice overlay culture system. (A) Representative images of neurons cultured for 18 or 48 h and high-magnification images of boxed areas (a-d). The percentages of multipolar cells with apical enrichment of F-actin are shown on the right. Data are presented as mean±s.e.m. $^{**}P<0.01$ by a two-tailed Student's *t*-test (n=5-8 slice cultures). (B) Representative images of control and LPA4 shRNA-introduced neurons cultured for 2 days. (C) The percentages of cells showing wide distribution of F-actin are shown. Data are presented as mean±s.e.m. $^{***}P<0.001$ by a two-tailed Student's *t*-test (n=7 or 8 slice cultures from two independent experiments). Scale bars: 20 µm; 10 µm in magnified images in A.

neocortex. Importantly, secreted from the marginal zone, Sema3A and reelin function as polarizing cues for migratory neurons *in vivo*. Interfering with Sema3A and reelin signaling pathway disrupts the normal apical positioning of centrosome/Golgi in multipolar neurons. This defect is accompanied with the production of both misoriented bipolar neurons and multipolar neurons (Chen et al., 2008; Jossin and Cooper, 2011; Shelly et al., 2011). In contrast, disruption of LPA-LPA4 signaling did not affect positioning of the centrosome/Golgi. Thus, the action of the LPA-LPA4 axis on the multipolar-to-bipolar transition is distinct and unique: it occurs after the positioning of the centrosome and Golgi, and affects specifically the pia-directed process. Thus, during the multipolar-to-bipolar transition, multipolar newborn cortical neurons reorient their centrosome/Golgi via extracellular polarizing factors such as Sema3A/reelin. Via LPA-LPA4 signaling that acts as a later morphogenic cue, they then form the pia-directed process and acquire the bipolar morphology.

Fliamin A downstream of the LPA/LPA4 axis in pia-directed process formation

Dynamic remodeling of the actin network occurs during the multipolar-to-bipolar transition (Fig. S7). Importantly, normal apical enrichment of F-actin within differentiating multipolar neurons is prevented by LPA4 depletion (Fig. 7). Instead, F-actin remained all over the cell. Furthermore, we identified the F-actin-binding protein FlnA as a key effector of the LPA-LPA4 cascade: FlnA is destabilized in LPA4-depleted cells and overexpression of FlnA rescues the pia-directed process formation as well as cortical radial migration and neuronal positioning. Remodeling of the cytoskeleton via FlnA upon LPA/LPA4 pathway activation is rather specific. Indeed, RhoA GTPase, which also impacts the actin network, was not activated in cortical neurons in which actin rearrangement occurs (Fig. S11). On the other hand, stabilization of microtubules, as assessed by levels of Ac-tub, has been reported to control multipolar-to-bipolar morphological transition of cortical neurons (Ip et al., 2012; Wu et al., 2012). In our hands, depletion of LPA4 did not affect the levels of Ac-tub in cortical neurons (Fig. S12). This result suggests that LPA-LPA4 signaling is unlikely to direct multipolar-to-bipolar morphological transition through microtubule stabilization and/or tubulin acetylation. Nevertheless, LPA4 could modulate microtubule dynamics via other mechanisms to induce this transition.

FlnA has been reported to contribute to VZ surface lining by rearranging the actin cytoskeleton and interacting with various extracellular matrix proteins (Carabalona et al., 2012; Feng et al., 2006; Sarkisian et al., 2006). Despite the expression of LPA4 in both neural progenitors and migrating neurons, LPA4-depletion by *in utero* electroporation (i.e. LPA4 depletion in progenitor cells) resulted in no disturbance of the VZ surface. This result suggests that the LPA-LPA4 pathway is unlikely to contribute to regulation of FlnA levels in progenitors. Thus, the FlnA stabilization mechanism reported herein is neuron specific. Further studies examining how LPA4 regulates FlnA level will lead to a better understanding of the stage-specific regulation/function of FlnA.

LPA production and source affecting neuronal morphogenesis in the developing neocortex

LPA is mainly generated through pathways involving PLA1/PLA2 and ATX (Aoki et al., 2008). We found that application of both ATX inhibitors (HA155 and PF8380) and a PLA1/2 inhibitor (MAFP)

Development (2018) 145, dev162529. doi:10.1242/dev.162529

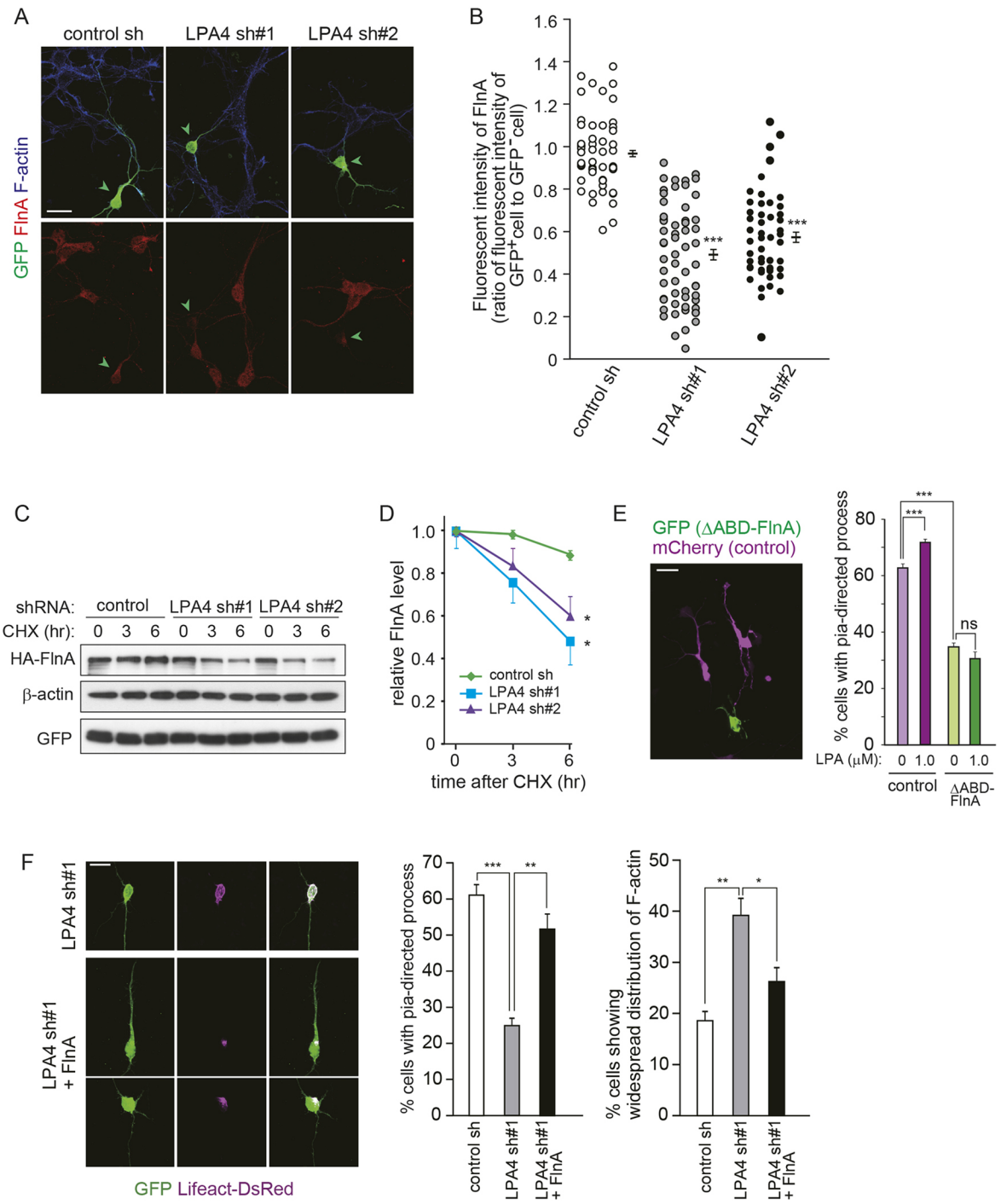

Fig. 8. Decreased levels of FlnA are coupled with LPA4 depletion. (A) Neocortical neuronal cultures were prepared from E16 brains that were electroporated at E14. The cells at 2 DIV were fixed and subjected to immunostaining using a FlnA antibody. Representative images are shown. Green arrowheads indicate GFP-positive cells. (B) Immunofluorescence intensity of FlnA in individual GFP-positive cells and that in nearby GFP-negative cells were measured, and the ratio of each intensity value is plotted. Horizontal line indicates the mean±s.e.m. ***P<0.001 by a two-tailed Welch's t-test (n=54, 59 and 51 cells for control, sh#1 and sh#2, respectively, from three independent experiments). (C) NIH3T3 cells were transiently transfected with plasmids expressing HA-FlnA and LPA4 shRNA. Forty-eight hours after the transfection, the cells were incubated in the presence of cycloheximide (CHX) for the indicated time periods. Then the cells were harvested, and the cell lysates were immunoblotted using antibodies indicated. (D) Quantified intensities of HA-FlnA were plotted as mean±s.e.m. by setting the peak value to 1. *P<0.05 by a two-tailed Student's t-test (n=3). (E) Representative image of GFP neurons and mCherry neurons, which were electroporated with indicated plasmids and subjected to slice overlay culture for 2 days. The percentages of cells with the pia-directed process in the total mCherry-labeled cells or GFP-labeled cells at the CP were calculated and are shown on the right. Data are presented as mean±s.e.m. ***P<0.001 by a two-tailed Student's t-test (n=7-17 slice cultures from more than three independent experiments). (F) Plasmids expressing GFP, LPA4 shRNA and FlnA as indicated were electroporated, together with the GFP- and Lifeact-DsRed-expressing plasmids, in E14 embryos. Neurons prepared from E16 brains were subjected to slice overlay culture for 2 days. Representative images of neurons are shown. The percentages of cells with the pia-directed process and showing wide distribution of F-actin are shown on the right. Data are presented as mean±s.e.m. *P<0.05, **P<0.01, ***P<0.001 by one-way ANOVA followed by Bonferroni's multiple comparison test (n=3-5 slice cultures). Scale bars: 20 µm.

Development (2018) 145, dev162529. doi:10.1242/dev.162529

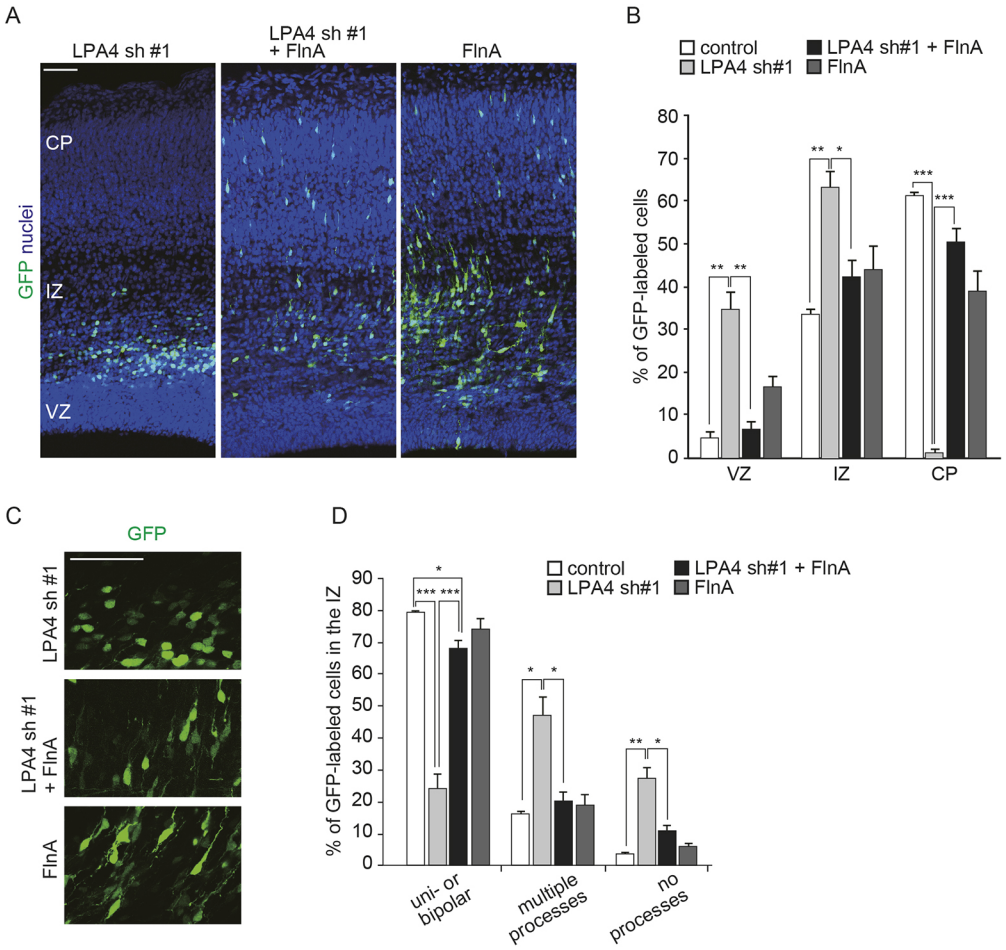

Fig. 9. Overexpression of FlnA reverses the effect of LPA4 knockdown on neuronal morphology and migration. Plasmids expressing GFP, LPA4 shRNA and FlnA were electroporated, together with the GFP-expressing plasmid, in E14 embryos, and the embryos were harvested at E17. Brain sections were immunostained with the antibody against GFP (green). Nuclei were stained with TO-PRO-3 iodide. (A) Representative images of GFP-labeled cells throughout the entire cerebral wall. (B) The percentages of GFP-labeled cells in the VZ, IZ and CP were calculated and are plotted as the mean±s.e.m. **P*<0.05, ***P*<0.01, ****P*<0.001 by one-way ANOVA followed by Bonferroni's multiple comparison test (*n*=3 or 4 brains; 1450, 1645, 1459 and 1393 cells were counted for control, sh#1, sh#1+FlnA and FlnA, respectively). (C) Magnified images of GFP-labeled cells in the IZ. (D) The percentage of GFP-labeled neurons with uni- or bipolar morphology, multiple (≥3) minor processes or no processes in the IZ was calculated and is plotted as mean±s.e.m. **P*<0.05, ***P*<0.01, ****P*<0.001 by one-way ANOVA followed by Bonferroni's multiple comparison test (*n*=3 or 4 brains; 211, 191, 272 and 223 cells were counted for control, sh#1, sh#1+FlnA and FlnA, respectively). Scale bars: 50 µm.

resulted in impaired formation of pia-directed process and altered neuronal migration. These observations indicate that PLA1/PLA2 and ATX are both involved in production of extracellular LPA to affect neuronal morphogenesis. Of note, depletion of ATX has little effect on neuronal migration (Greenman et al., 2015). As ATX is a secreted enzyme, ATX depletion could be rescued by ATX produced by neighboring cortical cells and/or a non-cortical source. In the present study, we used bath application of PF8380 to inhibit the ATX activity in the entire cultured cortex, thereby dissecting out roles of the ATX-LPA pathway in neuronal migration. Importantly, ATX is expressed in the CP and subplate (Greenman et al., 2015; Cheng et al., 2016), whereas PLA is present in cortical neurons (Kishimoto et al., 1999; Ong et al., 2010). In addition, LPA is present in the IZ and CP with enrichment around the CP and subplate in the neocortex at E16 (Cheng et al., 2016). LPA can also be synthesized and secreted by cortical neurons in culture (Fukushima et al., 2000). Considering these studies and our data, we provide a working model in which multipolar neurons in the SVZ and lower IZ are exposed to LPA produced in the SP/CP; upon LPA action on LPA4, these newborn neurons adopt a bipolar morphology and initiate radial migration from the IZ.

In conclusion, our study provides novel insights into the morphogenesis of newborn neocortical neurons and their migratory environment and ability. The identification of the LPA-LPA4-FlnA axis carries the hope of deciphering novel mechanisms underlying environmental regulation of neuronal morphogenesis and neuronal migration, which are central processes in corticogenesis.

MATERIALS AND METHODS

Animals

ICR mice were purchased from SLC (Hamamatsu, Japan) and were housed under a 12 h light-12 h dark cycle with *ad libitum* access to food and water. Both male and female mice were employed without distinction in all the experiments. All animal experiments were conducted in accordance with guidelines set by The University of Tokyo and approved (permit number 21-01) by the Committee on Animal Care and Use of the Graduate School of Science in The University of Tokyo.

Plasmids

pCAGIG plasmid (expressing GFP under the control of the CAG promoter), GFP-ΔABD-FlnA-expressing plasmid, HA-FlnA-expressing plasmid and pBS/U6 plasmid were kind gifts from Drs Takahiko Matsuda (Kyoto University, Japan), Makoto Sato (Osaka University, Japan), Thomas Stossel (Harvard Medical School, Boston, MA, USA) and Yang Shi (Harvard Medical School, Boston, MA, USA), respectively. For generating a plasmid expressing LPA4, mCherry and DsRed2-CentrinII under the control of CAG promotor, the full-length open reading frame of each gene was amplified by PCR with Pfu Turbo polymerase (Stratagene) and subcloned into the pCAGEN plasmid (a kind gift from Dr Takahiko Matsuda). Plasmids encoding silent mutation of LPA4 (LPA4-res) were generated using a QuikChange mutagenesis technique (Agilent Technologies) with primers 5′-catct atggg agcat gctgt ttctc acctg catca gtg-3′ (forward) and 5′-cactg atgca ggtga gaaac agcat gctcc catag atg-3′ (reverse). For HA-tagged LPA4, an oligonucleotide-encoding HA epitope sequence was fused to the 5′ end of the full-length LPA4 coding sequence. Plasmid expressing Lifeact-DsRed (Riedl et al., 2008) was generated by inserting the fragment encoding MGVADLIKKFESISKEE-DsRed into the pCAGEN plasmid. Plasmids encoding LPA4 shRNA were generated by inserting the annealed

Development (2018) 145, dev162529. doi:10.1242/dev.162529

oligonucleotides into the pBS/U6 plasmid (Sui et al., 2002). The target sequences for RNAi are as follows: for LPA4 shRNA#1, 5′-gggag caugc ucuuc cucac c-3′; for LPA4 shRNA#2, 5′-gggac ugcgu uccuc accaa c-3′.

Antibodies

Antibody against LPA4 was generated by Sigma Genosis as described below. Synthetic peptides corresponding to the amino acids Thr^{341}-Gln^{356} of LPA4 were conjugated to keyhole limpet hemocyanin and were injected into rabbits. LPA4 antibody was affinity-purified from the serum by a column coupled with immunogen peptides.

The following antibodies were used for immunostaining. Rabbit anti-LPA4 (1:100), rat anti-GFP (1:2000; 04434-34, Nakalai Tesque), rabbit anti-GFP (1:2000; A11122, Invitrogen), mouse anti-MAP2 (1:5000; ab11268, Abcam), mouse anti-Tuj1 (1:3000; MMS-435P, Covance), mouse anti-nestin (1:1000, 556309, BD Biosciences), rabbit anti-BLBP (1;1000, AB9558, Chemicon), rabbit anti-Pax6 (1:1000; PRB-278P, Covance), rabbit anti-Tbr2 (1:500; ab23345, Abcam), rabbit anti-Cux1 (1:100; sc-13024, Santa Cruz Biotechnology), mouse anti-GM130 (1:300, 610822, BD Biosciences), mouse anti-FlnA (1:100, ab80837, Abcam), mouse anti-acetylated tubulin (1:500, T6793, Sigma-Aldrich) and rabbit anti-cleaved caspase 3 (1:500; #9661, Cell Signaling Technology).

The following antibodies were used for immunoblotting and immunoprecipitation. Rabbit anti-GFP (1:2000; A11122, Invitrogen), rabbit anti-HA (1:1000, 561, MBL), mouse anti-FLAG (1:1000; F1804, Sigma-Aldrich) and mouse anti-β-actin (1:50,000; A1978, Sigma-Aldrich).

In utero electroporation

DNA solution in PBS containing 0.01% Fast Green was injected into the lateral ventricle of mouse embryos. Thereafter, electroporation (five 50 ms square pulse with 950 ms intervals; Nepa gene, CUY21-EDIT) was carried out with forceps-type electrodes (CUY650P5; Nepa gene) to introduce plasmids into neural progenitor cells in the VZ of the developing neocortex. Electroporation voltage used was 42V. Final concentrations of the plasmids used are as follows. Plasmids expressing GFP (pCAGIG: 2-5 µg/µl), mCherry (2 µg/µl), DsRed2-CentrinII (0.5 µg/µl), LPA4 with silent mutation (5 µg/µl), Lifeact-DsRed (0.5 µg/µl), LPA4 shRNA (1-2 µg/µl), HA-FlnA (8 µg/µl) and GFP-ΔABD-FlnA (5 µg/µl).

Immunohistochemistry

Brains were fixed with 4% paraformaldehyde in PBS for 30 min (for embryonic brains) or 2 h (for postnatal brains) at room temperature and cryoprotected in 30% sucrose in PBS overnight at 4°C. Thereafter, the brains were embedded in a solution of a 2:1 mixture of 30% sucrose/PBS and OCT compound (Sakura, Tokyo, Japan), frozen by liquid nitrogen and stored at −80°C until use. Thick cryosections (20 µm) were made. Brain sections were washed with PBS, incubated with blocking solution [3% (w/v) BSA, 5% (v/v) FBS and 0.2% (w/v) Triton X-100 in PBS] and then incubated with primary antibodies overnight at 4°C. The sections were then incubated with Alexa488/Cy3/Cy5-conjugated secondary antibodies overnight at 4°C and mounted in a Prolong Gold mounting solution (Invitrogen). Nuclei were visualized with TO-PRO-3 (Thermo Fisher Scientific). Images were obtained with a 63× objective (Plan-Apochromat; Zeiss) on Zeiss LSM 5 confocal microscope.

Cell culture and transfection

HEK293 and NIH3T3 cells were purchased from the European Collection of Authenticated Cell Cultures (ECACC). We did not authenticate the cell line in our lab. The lot was authenticated by ECACC before shipment. We did not test for mycoplasma contamination in our lab. The lot was tested at ECACC before shipment. HEK293 or NIH3T3 cells maintained in 10% FBS/DMEM were transiently transfected using Lipofectamin 3000 (Invitrogen) according to the manufacturer's instructions. Transfected cells were then cultured in 10% FBS/DMEM for 48 h. For detection of LPA4, the cells were serum starved overnight before the harvest. For inhibition of protein synthesis, cycloheximide (final concentration, 100 µM; Nacalai Tesque) was added to the culture medium. The cells were then subjected to immunoblotting, immunoprecipitation or immunocytochemistry.

Neocortical neuronal culture and immunocytochemistry

For neocortical neuronal culture, E14 embryos were electroporated with plasmids encoding GFP, mCherry, DsRed2-CentrinII, LPA4 shRNA and LPA4 with silence mutation. Forty-eight hours after electroporation, neocortical cells were prepared and cultured as described earlier (Asada et al., 2007). Cultured cortical neurons were fixed at 1 day *in vitro* (DIV; the plating day is defined as 0 DIV) or 2 DIV with 4% paraformaldehyde in PBS for 30 min at 37°C, permeabilized with 0.5% Triton X-100 in PBS for 5 min, blocked with 3% BSA/0.2% Triton X-100 in PBS and incubated with primary antibodies in the blocking solution at 4°C overnight. The coverslips were then incubated with Alexa488/Cy3/Cy5-conjugated secondary antibodies for 2 h at room temperature and mounted in a Prolong Gold mounting solution (Invitrogen). F-actin was visualized using acti-stain phalloidin (Cytoskeleton). Fluorescent images were obtained using Zeiss LSM5 confocal microscope.

Immunoprecipitation

The harvested cells were lysed in lysis buffer [20 mM Tris-HCl, 1% (vol/vol) Triton X-100, 10% (vol/vol) glycerol, 137 mM NaCl, 1 mM dithiothreitol, 2 mM EDTA, 50 mM NaF, 1 mM Na_3VO_4 and protease inhibitor cocktail (Complete, EDTA-free; Roche); pH 8.0 at 4°C]. After a 30 min incubation on ice, the cell lysates were centrifuged for 10 min at 20,000 ***g***, and the resultant supernatant was collected. The cell extracts were then incubated with 1.0 µg of a precipitating antibody at 4°C overnight, followed by incubation with 15 µl of protein G-Sepharose at 4°C for 3 h. The beads were washed three times with lysis buffer and subjected to immunoblotting.

LPA treatment, F-actin staining and active RhoA pull-down assay of cortical neurons

E16 neocortices were incubated in 1 ml HBSS (Invitrogen) containing papain (20 units; Roche), L-cystein (0.32 mg/ml) and 20 mM HEPES-NaOH (pH 7.4) for 30 min. The neocortices were rinsed twice with HBSS and dispersed with a fire-polished Pasteur pipet in Neurobasal media (Invitrogen) containing B27 (Invitrogen), glutamine and PenStrep. Neocortical cultures were treated at DIV1 with 1 µM LPA. At DIV1, almost all of the neocortical cells (>98%) were Tuj1-positive neurons. For F-actin staining, neurons were fixed with 4% paraformaldehyde/PBS for 20 min at 37°C. Neurons were then rinsed with PBS, followed by treatment with 0.5% Triton X-100/PBS for 5 min at room temperature. Thereafter, F-actin was visualized with acti-stain phalloidin (Cytoskeleton). RhoA activity was measured with a RhoA activation assay kit (Abcam) using neocortical cells prepared as above. NIH3T3 cells were serum starved in DMEM supplemented with 0.1% FBS for 24 h, prior to LPA treatment.

Slice overlay culture and time-lapse imaging

Acute brain slices (300 µm) of postnatal day 1 or 2 mouse brains were prepared as described previously (Asada and Sanada, 2010). Neocortical regions were dissected out from the slice and transferred onto a transparent porous membrane (1.0 µm pore size, BD Falcon; precoated with poly-D-lysine and laminin) in a 35 mm well containing culture media [F-12/DMEM supplemented with N2 and 5% horse serum (Invitrogen)]. Neocortical neuronal culture was prepared from E16 mouse brains as described above, and plating on top of cortical slices that were settled for 2 h after preparation. Three hours after the cell plating, culture membranes were transferred to the culture media without serum. For LPA/drug treatment, LPA (final concentration, 200 nM or 1 µM: Cayman Chemical), HA155 (final concentration, 1 µM: Sigma-Aldrich), PF8380 (final concentration, 1 µM: Sigma-Aldrich) and methyl arachidonyl fluorophosphates (MAFP) (final concentration, 10 µM: Cayman Chemical) were added to the media. Thirty-six to 48 h after the cell plating, neuronal cultures were fixed with 4% paraformaldehyde in PBS for 30 min at 37°C, then subjected to immunostaining.

For time-lapse imaging of Lifeact-DsRed, neuronal cultures were first treated with MAFP and PF8380 for 37 h to maintain and to synchronize them at the multipolar stage. Thereafter, LPA was supplemented to induce pia-directed process formation. Images of GFP and DsRed were then taken every 1-6 h for about 24 h. The experiments were designed to minimalize

phototoxicity but allowed us to clearly image the multipolar-to-bipolar transition. At each time-point, the Petri dishes with slice overlay culture were transferred from the CO_2 incubator to an Axio observer upright microscope (Carl Zeiss Microimaging), and images of GFP-expressing cells were collected with an AxioCam cooled CCD camera (Carl Zeiss Microimaging).

Slice culture

Plasmid expressing GFP was electroporated into E14 neocortices. Forty hours later, acute brain slices of electroporated brains were prepared using the method described above. Slices were cultured on a transparent porous membrane in a six-well culture plate containing culture medium (F-12/DMEM supplemented with N2 and B27) for 36 h. The reagents used were LPA (final concentration, 1 µM), PF8380 (final concentration, 1 µM) and MAFP (final concentration, 10 µM). Cultured slices were fixed in 4% paraformaldehyde and then subjected to immunostaining.

Statistical analysis

All bar graphs were plotted as mean±s.e.m. Direct comparisons were made using two-tailed Student's or Welch's *t*-test. One-way ANOVA followed by Bonferroni's multiple comparison test was used for experiments for three or more datasets. Repeat measures two-way ANOVAs were performed for comparisons of neuronal positioning of cortical slice cultures. These statistical analyses were performed using Microsoft Excel. The significance level was set at $P<0.05$ for all tests. No statistical methods were used to predetermine sample sizes but our sample sizes are similar to those generally employed in the field. The experiments were randomized, and data collection and analyses were performed blind to the experimental condition.

Acknowledgements

We thank Drs Takahiko Matsuda, Makoto Sato, Thomas Stossel and Yang Shi for plasmids.

Competing interests

The authors declare no competing or financial interests.

Author contributions

Conceptualization: N.K., K.S.; Investigation: N.K., A.T.; Writing - original draft: N.K., K.S.; Writing - review & editing: N.K., M.D.N., K.S.; Supervision: K.S.; Funding acquisition: N.K., K.S.

Funding

This work was supported in part by Grants-in-Aid for Scientific Research (C) (15K06697 and 18K06458 to N.K., and 17K07045 to K.S.) and by Grants-in-Aid for Scientific Research on Innovative Areas (17H05759 to K.S.) from the Ministry of Education, Culture, Sports, Science and Technology of Japan, and by research grants from the Mitsubishi Foundation, Takeda Science Foundation (N.K.), Naito Foundation (K.S.) and Canadian Institutes of Health Research (M.D.N.).

Supplementary information

Supplementary information available online at
http://dev.biologists.org/lookup/doi/10.1242/dev.162529.supplemental

References

Albers, H. M., Dong, A., van Meeteren, L. A., Egan, D. A., Sunkara, M., van Tilburg, E. W., Schuurman, K., van Tellingen, O., Morris, A. J., Smyth, S. S. et al. (2010). Boronic acid-based inhibitor of autotaxin reveals rapid turnover of LPA in the circulation. *Proc. Natl Acad. Sci. USA* **107**, 7257-7262.

Aoki, J., Inoue, A. and Okudaira, S. (2008). Two pathways for lysophosphatidic acid production. *Biochim. Biophys. Acta* **1781**, 513-518.

Asada, N. and Sanada, K. (2010). LKB1-mediated spatial control of GSK3beta and adenomatous polyposis coli contributes to centrosomal forward movement and neuronal migration in the developing neocortex. *J. Neurosci.* **30**, 8852-8865.

Asada, N., Sanada, K. and Fukada, Y. (2007). LKB1 regulates neuronal migration and neuronal differentiation in the developing neocortex through centrosomal positioning. *J. Neurosci.* **27**, 11769-11775.

Ayala, R., Shu, T. and Tsai, L.-H. (2007). Trekking across the brain: the journey of neuronal migration. *Cell* **128**, 29-43.

Bai, J., Ramos, R. L., Ackman, J. B., Thomas, A. M., Lee, R. V. and LoTurco, J. J. (2003). RNAi reveals doublecortin is required for radial migration in rat neocortex. *Nat. Neurosci.* **6**, 1277-1283.

Campbell, D. S. and Holt, C. E. (2003). Apoptotic pathway and MAPKs differentially regulate chemotropic responses of retinal growth cones. *Neuron* **37**, 939-952.

Carabalona, A., Beguin, S., Pallesi-Pocachard, E., Buhler, E., Pellegrino, C., Arnaud, K., Hubert, P., Oualha, M., Siffroi, J. P., Khantane, S. et al. (2012). A glial origin for periventricular nodular heterotopia caused by impaired expression of Filamin-A. *Hum. Mol. Genet.* **21**, 1004-1017.

Chen, G., Sima, J., Jin, M., Wang, K.-Y., Xue, X.-J., Zheng, W., Ding, Y.-Q. and Yuan, X.-B. (2008). Semaphorin-3A guides radial migration of cortical neurons during development. *Nat. Neurosci.* **11**, 36-44.

Cheng, J., Sahani, S., Hausrat, T. J., Yang, J.-W., Ji, H., Schmarowski, N., Endle, H., Liu, X., Li, Y., Böttche, R. et al. (2016). Precise somatotopic thalamocortical axon guidance depends on LPA-mediated PRG-2/Radixin signaling. *Neuron* **92**, 126-142.

Choi, J. W., Herr, D. R., Noguchi, K., Yung, Y. C., Lee, C.-W., Mutoh, T., Lin, M.-E., Teo, S. T., Park, K. E., Mosley, A. N. et al. (2010). LPA receptors: subtypes and biological actions. *Annu. Rev. Pharmacol. Toxicol.* **50**, 157-186.

Contos, J. J. A., Ishii, I., Fukushima, N., Kingsbury, M. A., Ye, X., Kawamura, S., Brown, J. H. and Chun, J. (2002). Characterization of lpa_2 (Edg4) and lpa_1/lpa_2 (Edg2/Edg4) lysophosphatidic acid receptor knockout mice: signaling deficits without obvious phenotypic abnormality attributable to lpa_2. *Mol. Cell. Biol.* **22**, 6921-6929.

Cooper, J. J. A. (2014). Molecules and mechanisms that regulate multipolar migration in the intermediate zone. *Front. Cell Neurosci.* **8**, 386.

Evsyukova, I., Plestant, C. and Anton, E. S. (2013). Integrative mechanisms of oriented neuronal migration in the developing brain. *Annu. Rev. Cell Dev. Biol.* **29**, 299-353.

Feng, Y., Chen, M. H., Moskowitz, I. P., Mendonza, A. M., Vidali, L., Nakamura, F., Kwiatkowski, D. J. and Walsh, C. A. (2006). Filamin A (FLNA) is required for cell-cell contact in vascular development and cardiac morphogenesis. *Proc. Natl. Acad. Sci. USA* **103**, 19836-19841.

Fukushima, N., Weiner, J. A. and Chun, J. (2000). Lysophosphatidic acid (LPA) is a novel extracellular regulator of cortical neuroblast morphology. *Dev. Biol.* **228**, 6-18.

Fukushima, N., Weiner, J. A., Kaushal, D., Contos, J. J. A., Rehen, S. K., Kingsbury, M. A., Kim, K. Y. and Chun, J. (2002). Lysophosphatidic acid influences the morphology and motility of young, postmitotic cortical neurons. *Mol. Cell. Neurosci.* **20**, 271-282.

Fukushima, N., Shano, S., Moriyama, R. and Chun, J. (2007). Lysophosphatidic acid stimulates neuronal differentiation of cortical neuroblasts through the LPA1-G(i/o) pathway. *Neurochem. Int.* **50**, 302-307.

Gierse, J., Thorarensen, A., Beltey, K., Bradshaw-Pierce, E., Cortes-Burgos, L., Hall, T., Johnston, A., Murphy, M., Nemirovskiy, O., Ogawa, S. et al. (2010). A novel autotaxin inhibitor reduces lysophosphatidic acid levels in plasma and the site of inflammation. *J. Pharmacol. Exp. Ther.* **334**, 310-317.

Greenman, R., Gorelik, A., Sapir, T., Baumgart, J., Zamor, V., Segal-Salto, M., Levin-Zaidman, S., Aidinis, V., Aoki, J., Nitsch, R. et al. (2015). Non-cell autonomous and non-catalytic activities of ATX in the developing brain. *Front. Neurosci.* **9**, 53.

Higgs, H. N. and Glomset, J. A. (1996). Purification and properties of a phosphatidic acid-preferring phospholipase A1 from bovine testis. Examination of the molecular basis of its activation. *J. Biol. Chem.* **271**, 10874-10883.

Ip, J. P. K., Shi, L., Chen, Y., Itoh, Y., Fu, W.-Y., Betz, A., Yung, W.-H., Gotoh, Y., Fu, A. K. Y. and Ip, N. Y. (2012). α2-chimaerin controls neuronal migration and functioning of the cerebral cortex through CRMP-2. *Nat. Neurosci.* **15**, 39-47.

Jossin, Y. and Cooper, J. A. (2011). Reelin, Rap1 and N-cadherin orient the migration of multipolar neurons in the developing neocortex. *Nat. Neurosci.* **14**, 697-703.

Kingsbury, M. A., Rehen, S. K., Contos, J. J. A., Higgins, C. M. and Chun, J. (2003). Non-proliferative effects of lysophosphatidic acid enhance cortical growth and folding. *Nat. Neurosci.* **6**, 1292-1299.

Kishimoto, K., Matsumura, K., Kataoka, Y., Morii, H. and Watanabe, Y. (1999). Localization of cytosolic phospholipase A2 messenger RNA mainly in neurons in the rat brain. *Neuroscience* **92**, 1061-1077.

Kriegstein, A. R. and Noctor, S. C. (2004). Patterns of neuronal migration in the embryonic cortex. *Trends Neurosci.* **27**, 392-399.

Lee, Z., Cheng, C.-T., Zhang, H., Subler, M. A., Wu, J., Mukherjee, A., Windle, J. J., Chen, C.-K. and Fang, X. (2008). Role of LPA4/p2y9/GPR23 in negative regulation of cell motility. *Mol. Biol. Cell* **19**, 5435-5445.

LoTurco, J. J. and Bai, J. (2006). The multipolar stage and disruptions in neuronal migration. *Trends Neurosci.* **29**, 407-413.

Lucas, K. K. and Dennis, E. A. (2005). Distinguishing phospholipase A2 types in biological samples by employing group-specific assays in the presence of inhibitors. *Prostaglandins Other Lipid Mediat.* **77**, 235-248.

Marín, O., Valiente, M., Ge, X. and Tsai, L.-H. (2010). Guiding neuronal cell migrations. *Cold Spring Harb. Perspect Biol.* **2**, a001834.

Nagano, T., Morikubo, S. and Sato, M. (2004). Filamin A and FILIP (Filamin A-Interacting Protein) regulate cell polarity and motility in neocortical subventricular and intermediate zones during radial migration. *J. Neurosci.* **24**, 9648-9657.

Nieto, M., Monuki, E. S., Tang, H., Imitola, J., Haubst, N., Khoury, S. J., Cunningham, J., Götz, M. and Walsh, C. A. (2004). Expression of Cux-1 and Cux-2 in the subventricular zone and upper layers II-IV of the cerebral cortex. *J. Comp. Neurol.* **479**, 168-180.

Noctor, S. C., Martínez-Cerdeño, V., Ivic, L. and Kriegstein, A. R. (2004). Cortical neurons arise in symmetric and asymmetric division zones and migrate through specific phases. *Nat. Neurosci.* **7**, 136-144.

Ong, W.-Y., Farooqui, T. and Farooqui, A. A. (2010). Involvement of cytosolic phospholipase A_2, calcium independent phospholipase A_2 and plasmalogen selective phospholipase A_2 in neurodegenerative and neuropsychiatric conditions. *Curr. Med. Chem.* **17**, 2746-2763.

Polleux, F., Morrow, T. and Ghosh, A. (2000). Semaphorin 3A is a chemoattractant for cortical apical dendrites. *Nature* **404**, 567-573.

Razinia, Z., Makela, T., Ylanne, J. and Calderwood, D. A. (2012). Filamins in mechanosensing and signaling. *Annu. Rev. Biophys.* **41**, 227-246.

Riedl, J., Crevenna, A. H., Kessenbrock, K., Yu, J. H., Neukirchen, D., Bista, M., Bradke, F., Jenne, D., Holak, T. A., Werb, Z. et al. (2008). Lifeact: a versatile marker to visualize F-actin. *Nat. Methods* **5**, 605-607.

Sarkisian, M. R., Bartley, C. M., Chi, H., Nakamura, F., Hashimoto-Torii, K., Torii, M., Flavell, R. A. and Rakic, P. (2006). MEKK4 signaling regulates filamin expression and neuronal migration. *Neuron* **52**, 789-801.

Shelly, M., Cancedda, L., Lim, B. K., Popescu, A. T., Cheng, P.-L., Gao, H. and Poo, M.-M. (2011). Semaphorin3A regulates neuronal polarization by suppressing axon formation and promoting dendrite growth. *Neuron* **71**, 433-446.

Stossel, T. P., Condeelis, J., Cooley, L., Hartwig, J. H., Noegel, A., Schleicher, M. and Shapiro, S. S. (2001). Filamins as integrators of cell mechanics and signalling. *Nat. Rev. Mol. Cell Biol.* **2**, 138-145.

Sui, G., Soohoo, C., Affar, B., Gay, F., Shi, Y., Forrester, W. C. and Shi, Y. (2002). A DNA vector-based RNAi technology to suppress gene expression in mammalian cells. *Proc. Natl. Acad. Sci. USA* **99**, 5515-5520.

Sumida, H., Noguchi, K., Kihara, Y., Abe, M., Yanagida, K., Hamano, F., Sato, S., Tamaki, K., Morishita, Y., Kano, M. R. et al. (2010). LPA4 regulates blood and lymphatic vessel formation during mouse embryogenesis. *Blood* **116**, 5060-5070.

Tabata , H. and Nakajima , K. (2003). Multipolar migration: the third mode of radial neuronal migration in the developing cerebral cortex. *J. Neurosci.* **23**, 9996-10001.

Tokumura, A. (1995). A family of phospholipid autacoids: occurrence, metabolism and bioactions. *Prog. Lipid Res.* **34**, 151-184.

Tsai, L.-H. and Gleeson, J. G. (2005). Nucleokinesis in neuronal migration. *Neuron* **46**, 383-388.

Wu, Q.-F., Yang, L., Li, S., Wang, Q., Yuan, X.-B., Gao, X., Bao, L. and Zhang, X. (2012). Fibroblast growth factor 13 is a microtubule-stabilizing protein regulating neuronal polarization and migration. *Cell* **149**, 1549-1564.

Young-Pearse, T. L., Bai, J., Chang, R., Zheng, J. B., LoTurco, J. J. and Selkoe, D. J. (2007). A critical function for beta-amyloid precursor protein in neuronal migration revealed by in utero RNA interference. *J. Neurosci.* **27**, 14459-14469.

Yung, Y. C., Stoddard, N. C., Mirendil, H. and Chun, J. (2015). Lysophosphatidic Acid signaling in the nervous system. *Neuron* **85**, 669-682.

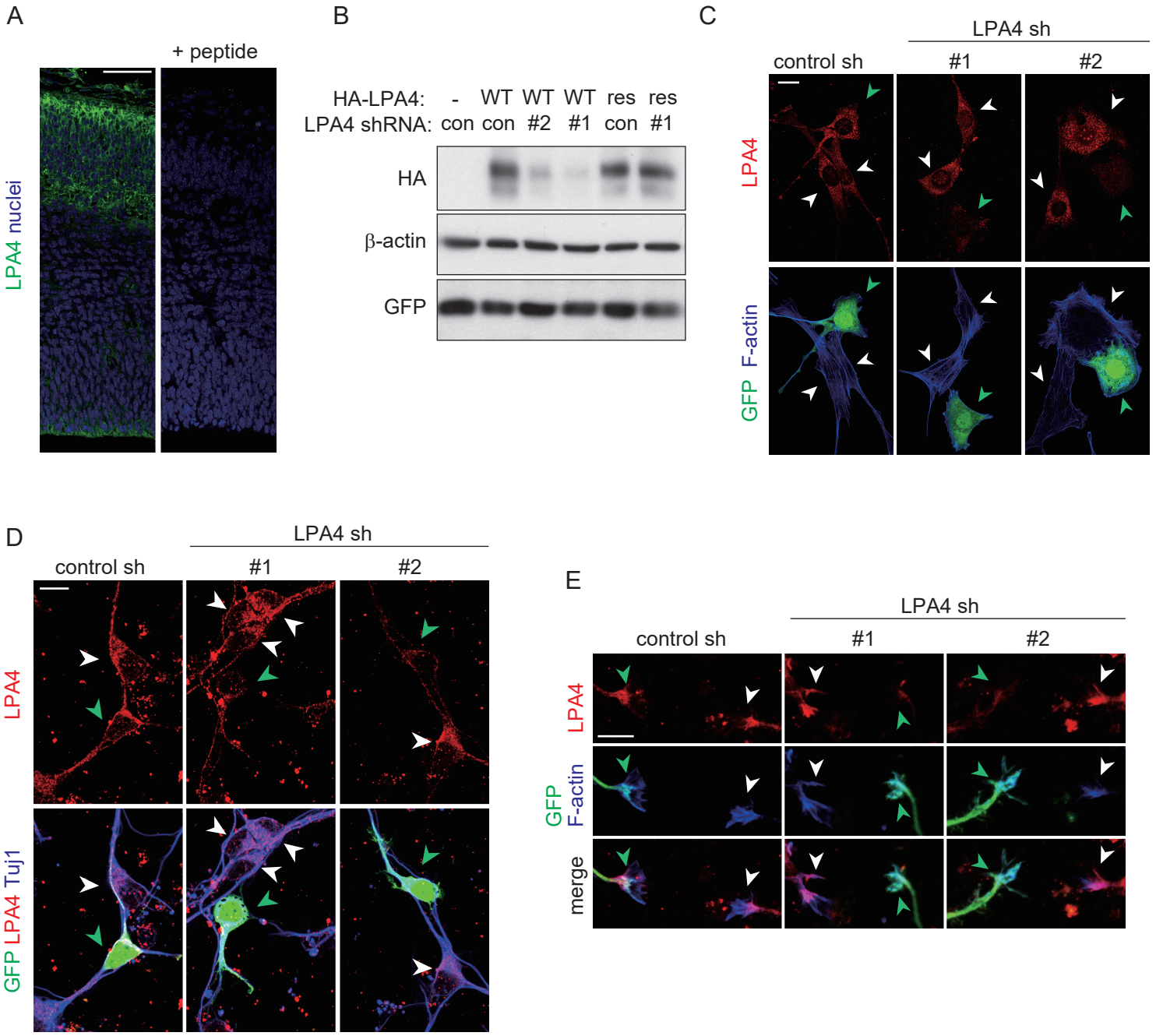

Figure S1. Validation of the LPA4 antibody and LPA4 shRNA plasmids.

(A) Images of E14 neocortical sections immunostained with anti-LPA4 antibody (left). The immunoreactivity of LPA4 is diminished by pre-incubation of the antibody with its peptide immunogen (right). Nuclei were stained with TO-PRO-3 iodide. (B) HEK293 cells were transiently transfected with plasmids indicated, together with the GFP-expressing plasmid. The cell lysate was prepared (48 hours later), and subjected to immunoblotting with antibodies against HA, β-actin and GFP. GFP serves as transfection control. (C) NIH3T3 cells were transiently transfected with either control shRNA plasmid or LPA4 shRNA plasmids, together with the GFP plasmid. Forty-eight hours after the transfection, cells were fixed and immunostained with antibodies against GFP and LPA4. F-actin was stained with Acti-stain phalloidin. Representative images are shown. Green and white arrowheads indicate GFP-positive and GFP-negative cells, respectively. (D, E) Plasmids expressing LPA4 shRNA were electroporated, together with the GFP-expressing plasmid, in E14 embryos. Neocortical cell cultures were prepared from E16 brains, and the DIV2 cells were immunostained with antibodies against GFP and LPA4. F-actin was stained with Acti-stain phalloidin. Representative images of cell somata (D) and neurite tips (E) are shown. Green and white arrowheads indicate GFP-positive and GFP-negative neurons, respectively. Scale bars: 50 μm (A), 20 μm (C), and 10 μm (D, E).

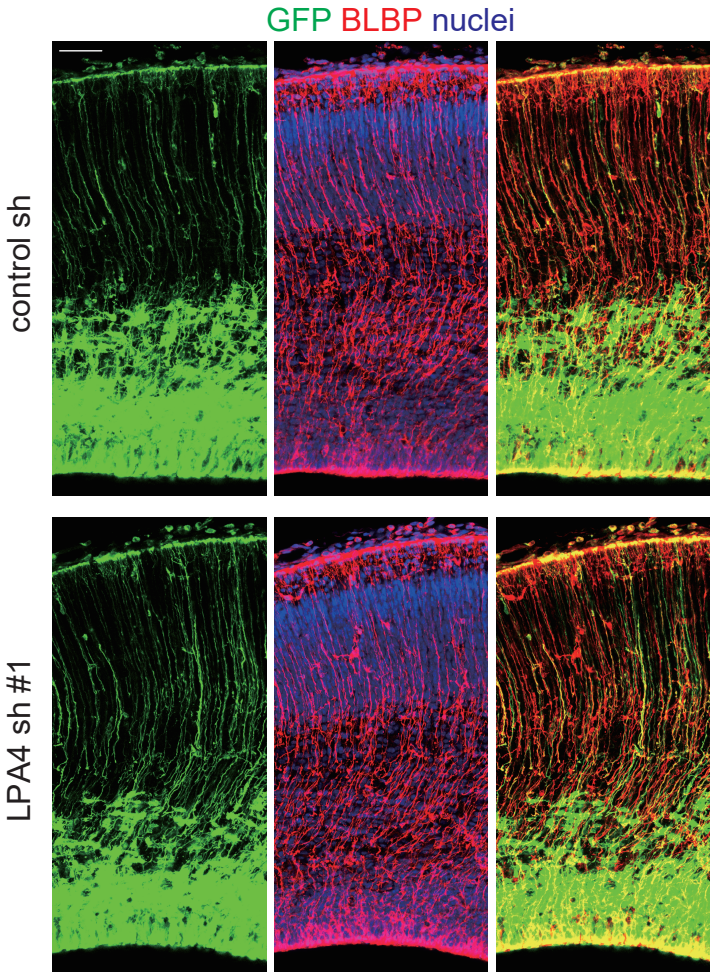

Figure S2. Knockdown of LPA4 does not affect radial fibers of radial glial cells.

Plasmids expressing GFP and LPA4 shRNA were electroporated in E14 embryos, and the embryos were harvested at E16. Representative images of the neocortical sections immunostained with a BLBP antibody. Both control brains and LPA4 shRNA-introduced brains show similar radial pattern of the GFP-labeled radial fibers. Scal bar: 50 μm.

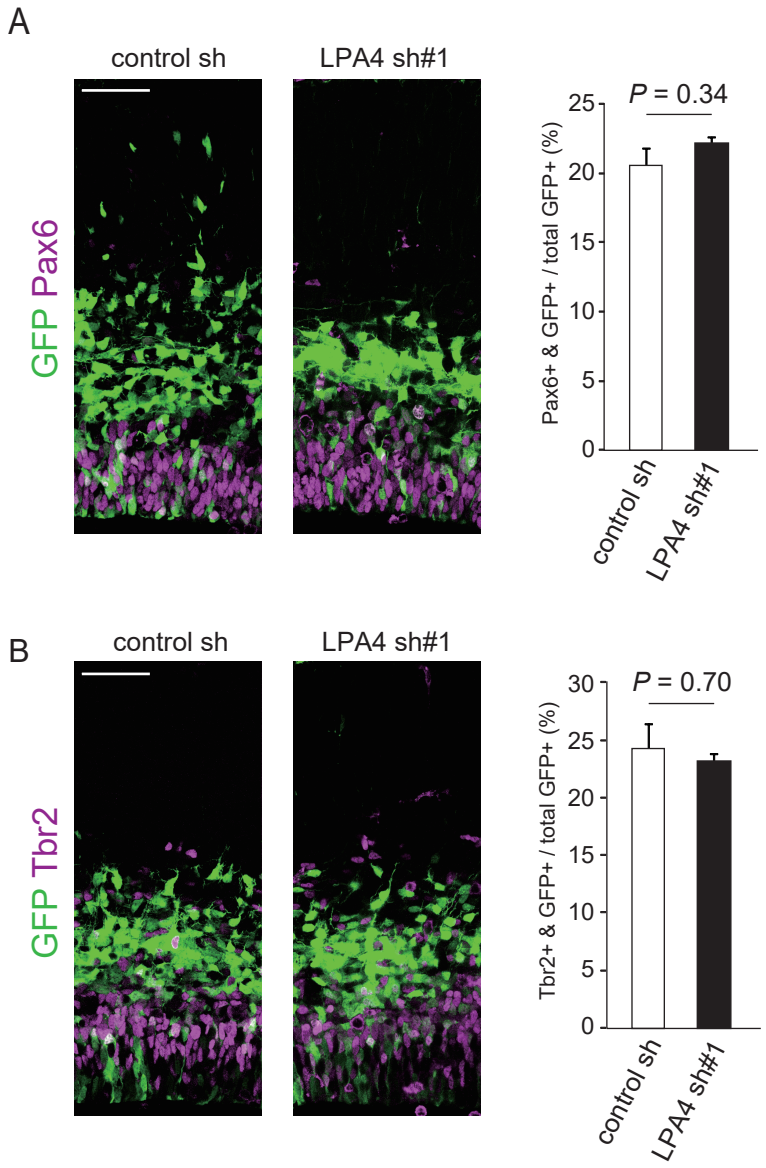

Figure S3. Knockdown of LPA4 does not affect neurogenesis.

The LPA4 shRNA plasmid was electroporated, together with the GFP-expressing plasmid, into E13 embryos. E15 brain sections were immunostained with antibodies against Pax6 (A) or Tbr2 (B). Representative images are shown. Quantifications of fraction of GFP-positive cells that were also positive to Pax6 and Tbr2 are shown to the right. Data are presented as mean ± SEM (n = 3-4 brains for each group. For Pax6, 834 and 730 cell were counted for control and sh#1, respectively. For Tbr2, 928 and 964 cell were counted for control and sh#1, respectively.). Scale bars: 50 μm.

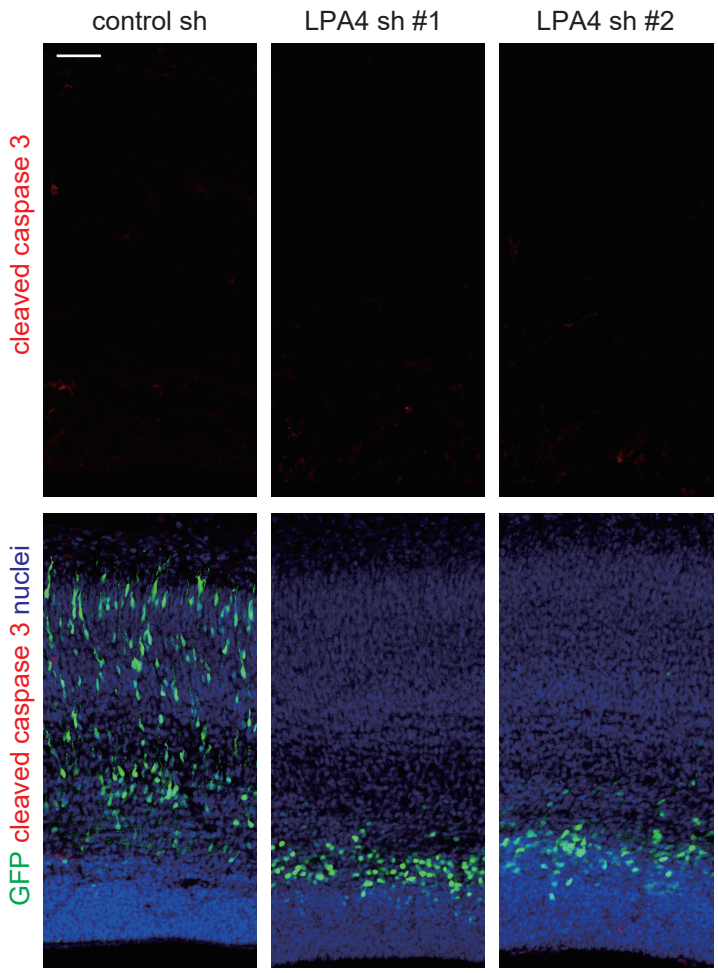

Figure S4. Introduction of LPA4 shRNA does not induce apoptotic cell death.

Plasmids indicated were electroporated, together with the GFP-expressing plasmid, in E14 embryos. The E17 brain sections were then immunostained with an antibody against cleaved caspase 3. Nuclei were stained with TO-PRO-3 iodide. Images of the entire cerebral wall are shown. Scale bar: 50 μm.

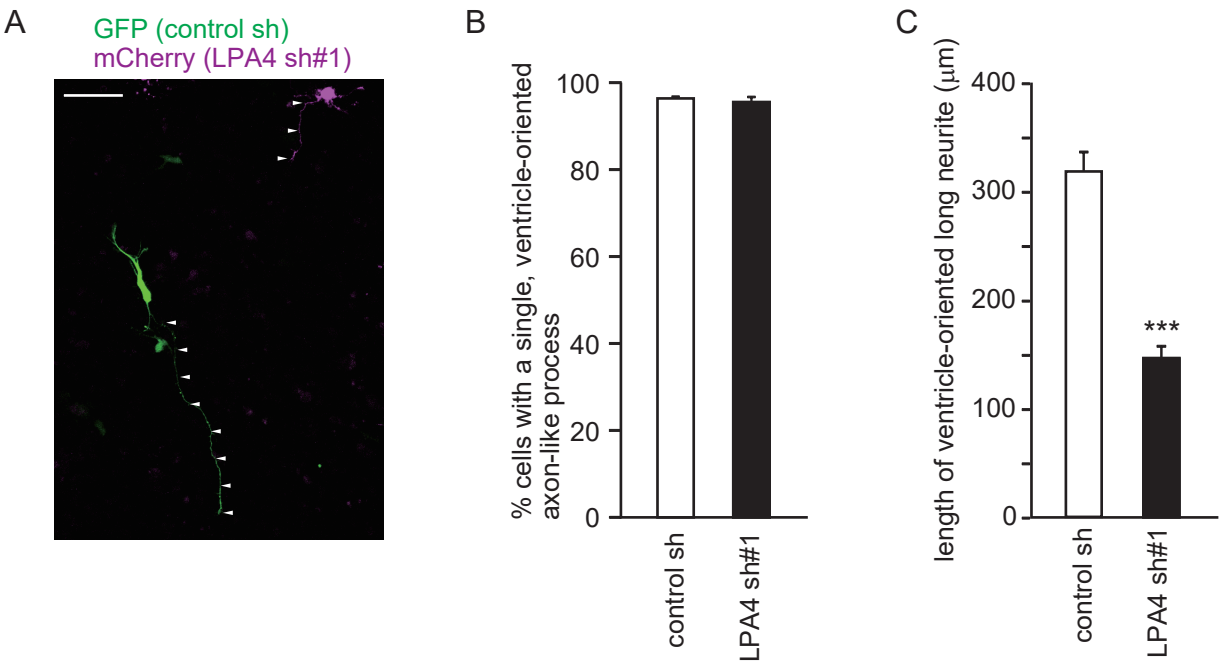

Figure S5. LPA4-depleted neurons extend axons.

(A) Representative images of a control shRNA-introduced GFP neuron and a LPA4 shRNA-introduced mCherry neuron in slice overlay culture are shown. (B) The percentages of cells with a single, ventricle-directed axon-like process in the total mCherry-labeled cells or GFP-labeled cells at the CP are shown. (C) The length of the ventricle-oriented, axon-like neurite (indicated by arrowheads) was measured and is presented as mean ± SEM. ***P < 0.001 by a two-tailed Welch's t-test (n = 30 and 38 cells for control sh and LPA4 sh#1 from three independent experiments). Scale bar: 50 μm.

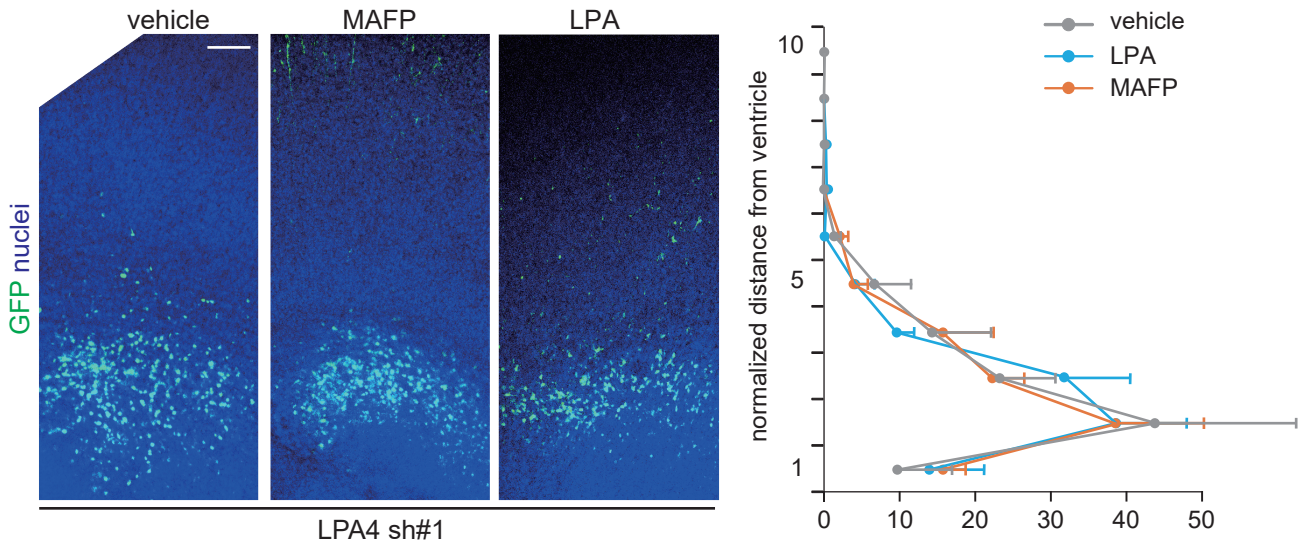

Figure S6. Positioning of LPA4-depleted neurons is not further influenced by LPA and LPA synthetic inhibitor.

Plasmids expressing GFP and LPA4 shRNA#1 was electroporated in E14 embryos. Acute brain slices were prepared from E16 brains and cultured for 36 hours. The cultures were then immunostained with an antibody against GFP (green). Nuclei were stained with TO-PRO-3 iodide. Representative images of GFP-labeled cells throughout the entire cerebral wall are shown to the left. Distributions of GFP-expressing cells along the radial axis under different treatments are shown to the right. Scale bar: 100 μm.

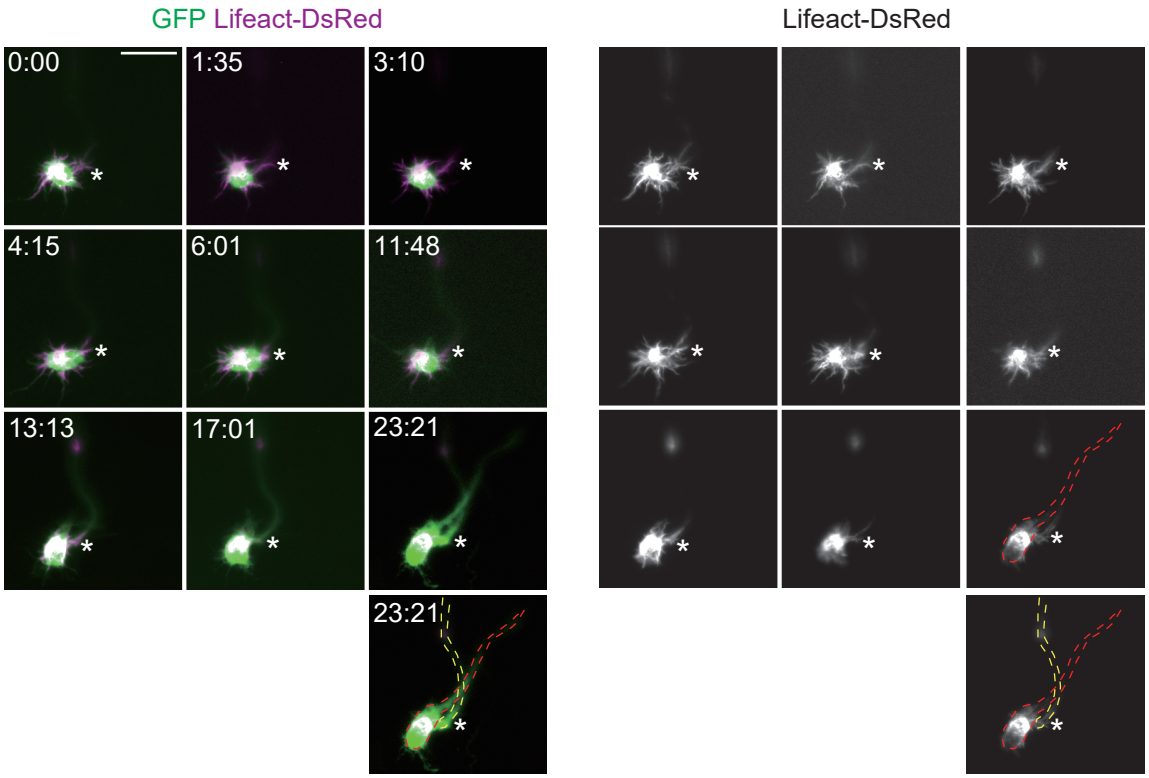

Figure S7. Time-lapse imaging of neurons during multipolar-to-bipolar transition in slice overlay system.

Plasmids expressing GFP and Lifeact-DsRed were electroporated in E14 embryos. Neuronal cultures were prepared from E16 brains, and then subjected to slice overlay cultures. Time-lapse images of electroporated neurons overlaid on neocortical slices were carried out according to the methods. Time is denoted as hours:minutes in the top of each panel. Asterisks indicate immunofluorescence signals of an axon from a neighboring cell. The cell soma and apical process of the focused cell (red) and an axon of the neighboring cell (yellow) are outlined with dashed lines in the last panel. Scale bar: 20 μm.

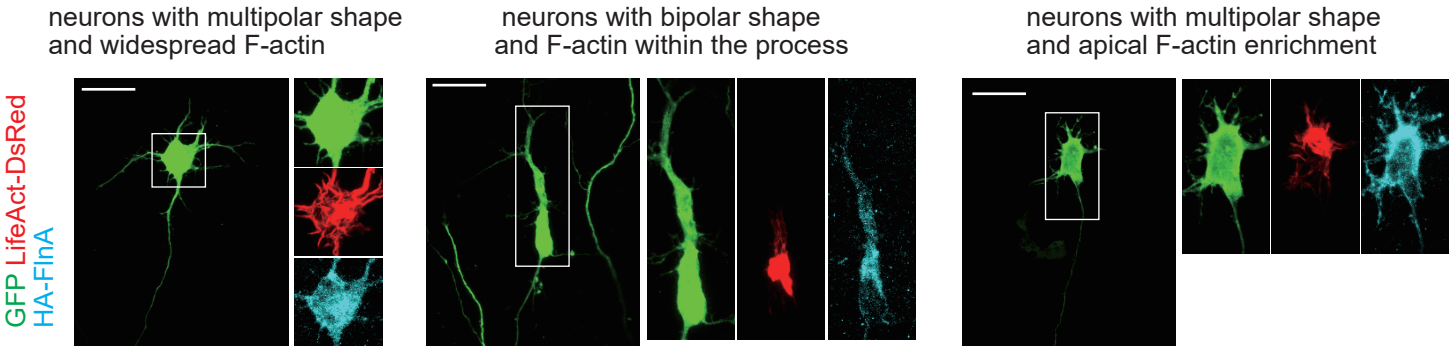

Figure S8. Subcellular localization of FlnA in cortical neurons in slice overlay system.

Plasmids expressing GFP and HA-FlnA were electroporated, together with the Lifeact-DsRed-expressing plasmids, in E14 embryos. Neurons prepared from E16 brains were subjected to slice overlay culture for two days. The cultures were then immunostained with an antibody against GFP and HA. Shown are representative images of neurons with multipolar shape and widespread F-actin distribution (right), neurons with bipolar shape and F-actin within the process (mid), and neurons with multipolar shape and apical F-actin enrichment. Scale bars: 20 μm.

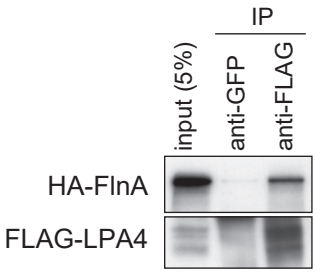

Fig. S9. LPA4 associates with FlnA.

HEK293 cells were transiently transfected with plasmids expressing LPA4 and FlnA. The cell lysates were prepared 48 hours after transfection and subjected to immunoprecipitation with antibodies indicated. The immunoprecipitates were then immunoblotted with antibodies against HA and FLAG as indicated.

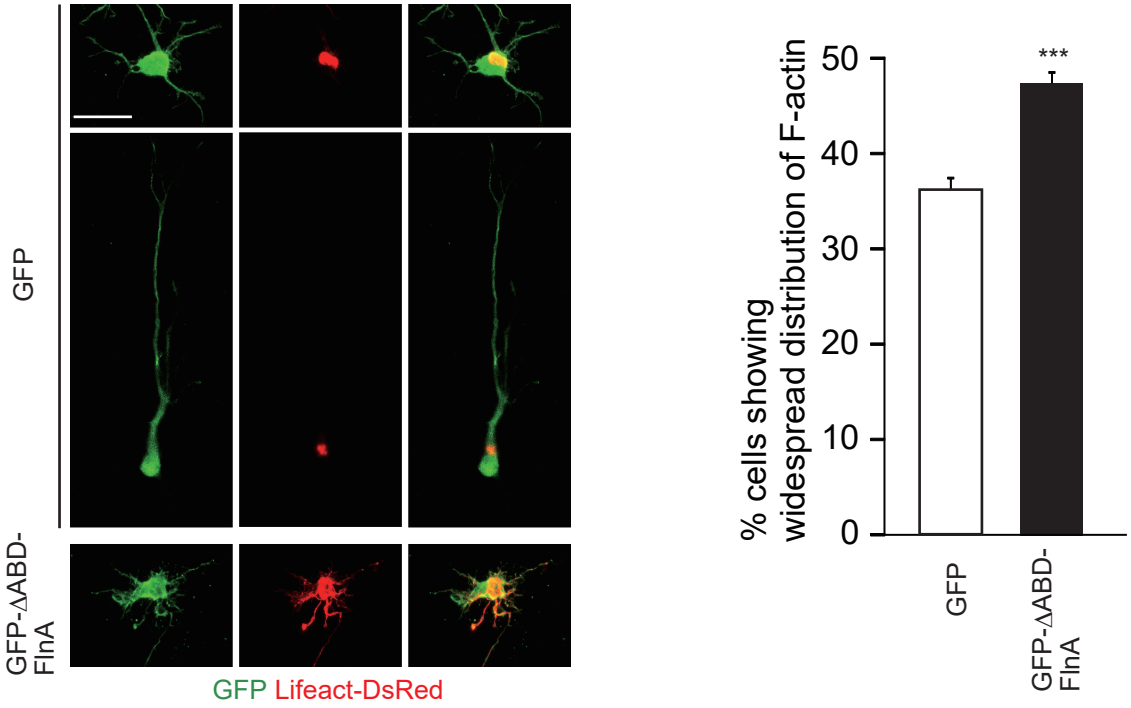

Figure S10. Dominant negative form of FlnA disturbs the accumulation of F-actin.

Plasmids expressing GFP or GFP-ΔABD-FlnA as indicated were electroporated, together with the Lifeact-DsRed-expressing plasmids, in E14 embryos. Neurons prepared from E16 brains were subjected to slice overlay culture for two days. Representative images of neurons were shown. The percentages of cells showing wide distribution of F-actin are shown to the right. Data are presented as mean ± SEM. ***P < 0.001 by a two-tailed Student's t-test (n = 6 and 10 slice cultures for control and ΔABD-FlnA, respectively). Scale bar: 20 μm.

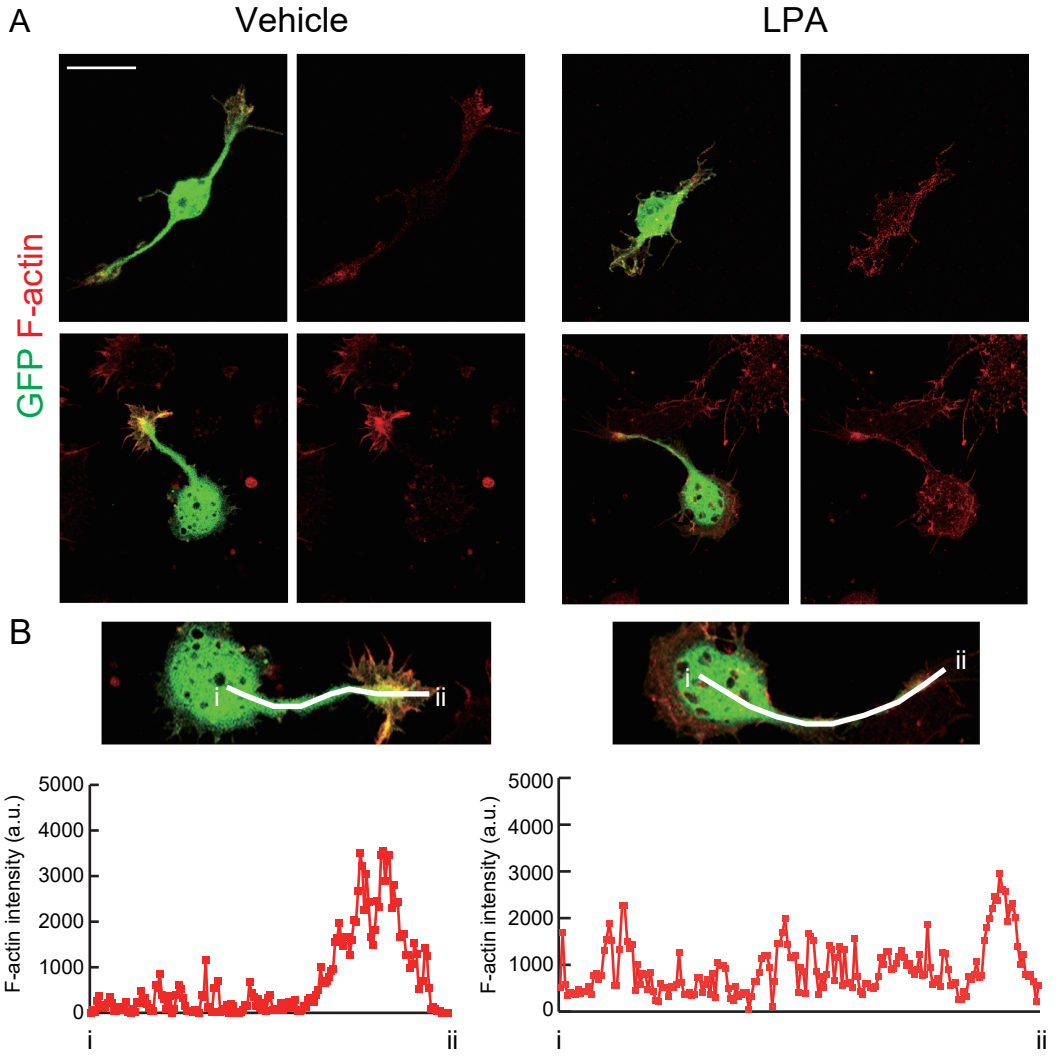

Figure S11. RhoA is not activated in neocortical neurons upon LPA treatment.

(A) Neurons were prepared from E16 cortices electroporated with GFP at E14 and cultured. At DIV2, neurons were treated with LPA for 20 min and subjected to F-actin staining. Representative images of GFP-labeled cells (with one or two thick processes) treated with or without LPA are shown. (B) Magnified images of GFP-labeled cells in (A). The graphs below the panels are the quantification of F-actin signals (a.u., arbitatory units) from i to ii (indicated with lines). In neocortical cells, F-actin is enriched within the process (59 out of the 65 GFP-labeled cells with one or more thick processes), whereas the enrichment becomes attenuated upon LPA treatment (21 out of the 48 GFP-labeled cells with one or more thick processes). (C) Neurons treated with LPA for indicated time were subjected to active RhoA pull-down assay. Active RhoA (RhoA GTP) pulled down with Rhotekin-agarose as well as total RhoA (1% lysate used for the pull-down assay) were visualized by immunoblotting with a RhoA antibody. As a control, NIH3T3 cells that were serum-starved for 24 hours prior to LPA treatment were subjected to active RhoA pull-down assay. (D) Quantified intensities of RhoA GTP (relative to those of 1% input) were plotted as means ± SEM. *P < 0.05 by a two-tailed Student's t-test (n =3). Scale bar: 20 μm.

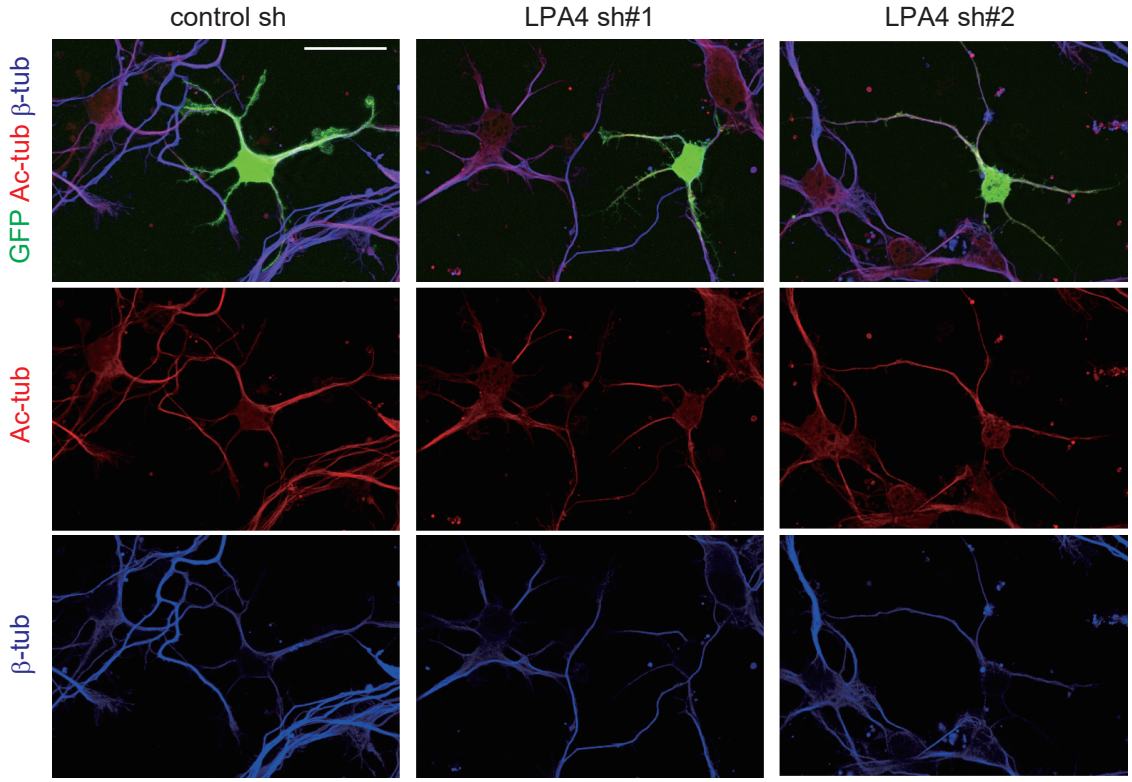

Fig. S12. Knockdown of LPA4 does not affect expression of acetylated-tubulin.

Neocortical neuronal cultures were prepared from E16 brains that were electroporated with GFP- and shRNA-expressing plasmids at E14. The cells at 2 DIV were fixed and subjected to immunostaining with antibodies against Acetylated-tubulin and beta-tubulin. Scale bar: 20 μm.